Chapter 3

Influence of Molecular Dipoles on the photoluminescence and Electroluminescence of Dipolar Donor-Acceptor-Substituted Spirobifluorene Fluorophores

3-1 Introduction

3-1-1 Short Introduction

Spirobifluorenes are a class of unique molecules which includes a rigid and non-planar linkage (spiro-junction) of two aromatic chromophores or fluorophores.[1] Such a special molecular framework does not allow an tight molecular packing, and the most porous network constructed from small molecules has been reported with spirobifluorenes.[1, 2]   On the other hand, the rigid and orthogonal structure of spirobifluorenes leads to a molecular entanglement in the solid state that prevents crystallization.   Amorphous thin films with high morphological stability due to the high glass transition temperatures (T_gs) often can be anticipated from spirobifluorene materials.[1, 3]   Amorphous materials with high morphological stability are highly demanded in the organic light-emitting diodes (OLEDs) because they have a higher chance to reinforce critical factors such as the operational lifetime, efficiency, and brightness of electroluminescence (EL).   Many spirobifluorene materials exhibit limited fluorescence quenching in solid state, which is a great advantage in the application of OLEDs.[1, 4]

From a chemical point of view, the common feature of many spiro-linked compounds synthesized so far is the central core of spirobifluorene, which is substituted with same or different substituents in the 2,2' and 7,7' positions as shown in **Figure 3-1**.   There currently exist several pathways to the synthesis of spiro-linked functional materials, whereas the choice of the right pathway depends on the desired substitution pattern.   Compounds, which

are fully symmetrically substituted in all four para positions, i.e., $R_1 = R_2 = R_3 = R_4$, are generally synthesized from spirobifluorene itself, such as 2,2',7,7'-tertabromo-9,9'-spirobifluorene.[5]   In the case of the unsymmetrical compounds, in which $R_1 = R_2 \neq R_3 = R_4$, a more complex strategy has to be applied, such as 2,7-dibromo-9,9'-spirobifluorene.[6]   The other kind of unsymmetrical spiro compounds, in which $R_1 = R_3 \neq R_2 = R_4$, can be accessed by direct substitution of spirobifluorene provided that the first two groups entering in the 2 and 2' positions deactivate the 7 and 7' positions, such as 2,2'-dinitro -9,9'-spirobifluorene[7] or 2,2'-diacetyl-9,9'-spirobifluorenes[8]. In this way, a subsequent substitution in these positions can be controlled as we wish.
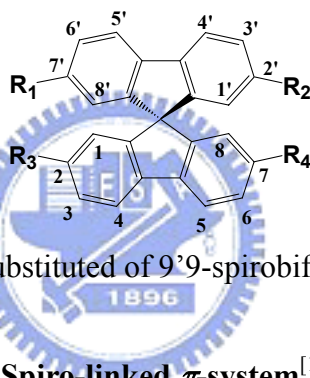

Figure 3-1. General structure of substituted of 9'9-spirobifluorene.

3-1-2 Electronic Coupling of the Spiro-linked π-system[1]

The electronic independence of two molecular halves in spriobifluorene can be understood by the perpendicular arrangement of two π-conjugated.[9]   When both of two molecular halves are in the ground state, the only electronic nodal plane of HOMO is the plane of each π-conjugation.   Across molecular halves π-interaction is prevented because of the symmetry mismatch of the wave functions.   On the other hand, higher π-orbitals LUMO may exhibit a second nodal plane perpendicular to the first one but parallel to the plane of the second molecular halve. The 4-fold symmetry of these molecular orbitals allows an interaction of both molecular halves (**Figure 3-2**).
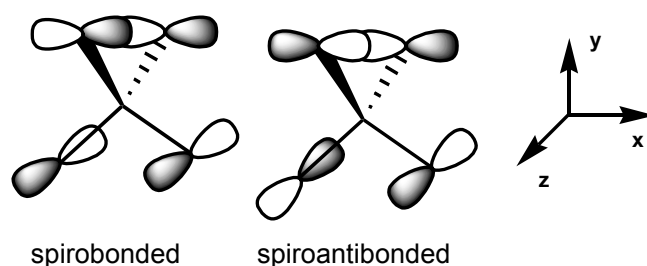
Figure 3-2. Model of spiro conjugation of molecular orbitals. The upper chromophore lies in the y-z plane, the lower chromophore in the x-y plane.[10]

In past 30 years, there are only few theoretical calculation applied on intramolecular interaction of two molecular halves of spriobifluorene. In 1995, Niels A. van Dantzig *et al.* reported that no electronic coupling and no corresponding exciton splitting of 9,9'-spirobifluorene were detected in the zero-point level of the S_1 state because of the symmetry of the structure. However, vibronic coupling interaction between two molecular halves has reported when the higher vibrational levels were excited.[11] The excitation energy transfer from vibrationally excited states between two identical molecular halves of 2,2',7,7'-tetrakis(biphenyl-4-yl)-9,9'-spirobifluorene (Spiro-6P) was demonstrated by Schartel et al. by means of fluorescence polarization spectroscopy.[12] Yip *et al.* estimated the rate of symmetry-forbidden but vibronically allowed energy transfer of spirofluorenephenanthrene and spirofluorenenaphthalene between spiro-linked donor-acceptor pairs to be on the order of 1×10^{12} s^{-1}.[13] Salbeck and co-works investigated the electronic and optical properties of the spiro molecules, 2,2'-bis(5-(4-tert-butylphenyl)-1,3,4-oxadiazol-2-yl)-9,9'-spirobifluorene (Spiro-PBD), and 2,2',7,7'-tetrakis(biphenyl-4-yl)-9,9'-spirobifluorene (Spiro-6P) by photoelectron spectroscopy, Raman spectroscopy, spectroscopic ellipsometry and quantum-chemical calculation in 1997.[14] Although two molecular halves are perpendicular to each other, there is slight interaction at the spiro-center. The interaction leads to a splitting of some of the orbitals (with reference to the orbitals of two separate molecules). In more practical terms it means that chemistry involving either branch is dependent on the other branch. Overall, the approach towards spiro type molecules to

increase solubility and to stabilize the amorphous solid state but keep the electronic and optical independncy of individual molecular halves can be considered a success.
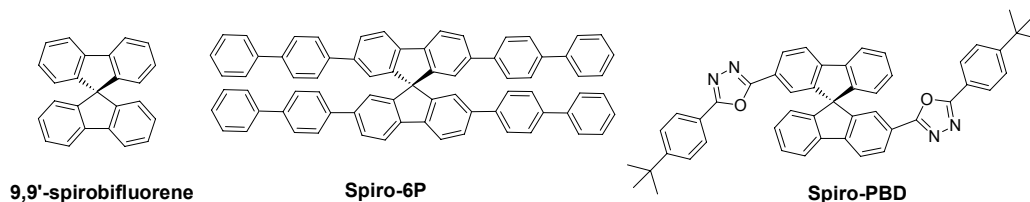

Figure 3-3. The chemical structures 9'9'-spirobifluorene, Spiro-6P and Spiro-PBD**.**
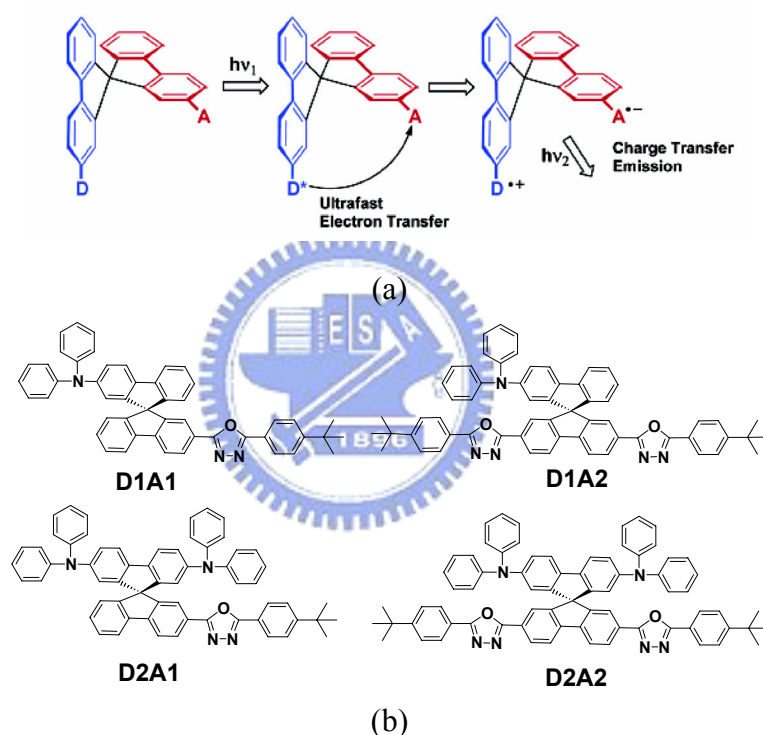

(a)

(b)

Figure 3-4. (a) Photoinduced electron transfer (PET) from the donor to the acceptor of spirobifluorene. (Reprinted from ref 15) (b) The chemical structures D1A1, D1A2, D2A1 and D2A2.[15]

In 2006, Wong et al investigated a series of spirobifluorene-bridged bipolar compounds consisting of electron-donating (triarylamine) and electron-accepting (1,3,4-oxadiazole) molecular halves. For these bipolar spirobifluorene molecules, photoinduced electron transfer (PET) from the donor half to the acceptor half was observed even in highly dilute solution (**Figure 3-4(a)**). A time constant of 430 fs was measured for the PET in D2A1 (460

nm). Whereas a similar time constant of 410 fs was obtained for D1A1, the electron transfer of compounds with two oxadiazole moieties as acceptors, D1A2 and D2A2, is substantially faster (< 150 fs).[15]
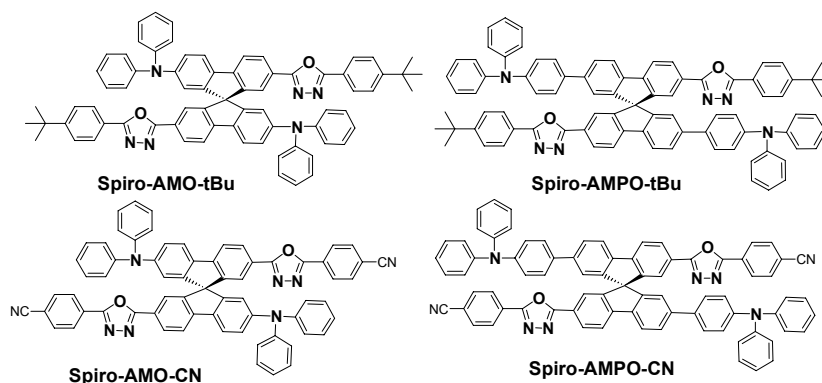

Figure 3-5. The chemical structures Spiro-AMO-tBu, Spiro-AMPO-tBu, Spiro-AMO-CN and Spiro-AMPO-CN.

In 2003, Salbeck et al synthesized a different type of spirobifluorene-bridged compounds bearing electron-donating groups (triarylamine) in 2,2'-positions and electron-accepting groups (1,3,4-oxadiazole) in 7,7'-positions (**Figure 3-5**).[16]   The high T_g between 165 and 212 ^{o}C demonstrated the high morphologic stability of the amorphous phase in a thermal vaccum-deposited film.   The solid state emission λ_{max} of these spiro compounds were detected at 477 nm of spiro-AMO-tBu, 483 nm for spiro-AMPO-tBu , 526 nm for spiro-AMO-CN, and 524 nm for spiro-AMPO-CN, respectively.   Since then, there is no more investigation of electronic interaction between the donor-acceptor spiro-linked π-system.

3-2 Motivation of research

A rare red fluorophore that is exceptionally efficient for non-dopant red OLEDs of 2-donor-7-acceptor-spirobifluorene, **PhSPDCV** was reported in Chapter 2. Non-dopant red OLEDs are extremely difficult to come by due to the lack of materials of which fluorescence

is not concentration quenching in solid state.[17] A novel fluorophore of **BisPhSPDCV** (Scheme 3-1) that contains two equivalent chormophores compare to **PhSPDCV** was expected to be a more efficient material for non-dopant red OLEDs. Accordingly, a series of 2-donor-7-acceptor-spirobifluorene compounds and 2,2'-bisdonor-7,7'-bisacceptor-spirobifluorene compounds are designed and synthesis (the retrosynthesis was showed in Scheme 3-1). Their physical properties, including dipole moment from quantum chemistry calculation, emission solvatochromism, fluorescence quantum yield (Φ_f) as well as EL are examined and compared in details.

Scheme 3-1

**The retrosynthesis of DonorSPAcceptor and BisDonorSPAcceptor**
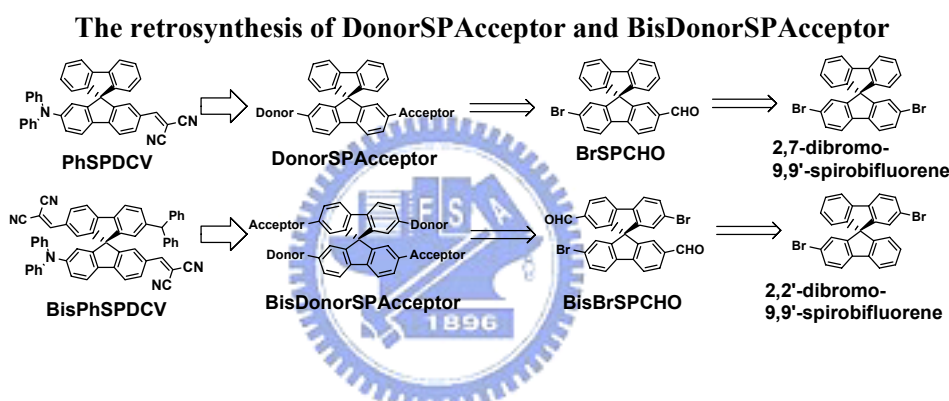
Although there are abundant optical and electronic molecular materials or polymers that are derived from 2,7-dibromo-9,9'-spirobifluorene,[1b, 4e-i, 6b, 18] very few materials originate from the closely related isomer 2,2'-dibromo-9,9'-spirobifluorene.[4b, 16b, 19] This drastic difference is mainly due to the easy preparation of 2,7-dibromo-9,9'-spirobifluorene, which is readily synthesized from 2,7-dibromo-9-fluorenone by reacting with a Grinard reagent of 2-bromobiphenyl.[6b] According to both literature and patent, 2,2'-dibromo-9,9'-spirofluorene can be prepared by direct bromination of 9,9'-spirobifluorene in the presence of a catalytic amount of ferric chloride by Sutcliffe et al and salbeck *et al.* (Scheme 3-2).[6a, 20] This and similar procedures were confirmed by other groups of Pei *et al.* and Park *et al.* They reported the synthesis with a isolated yield of 88%[6c] and 81%,[21] respectively. The ^{1}H-NMR spectrum of 2,2'-dibromo-9,9'-spirobifluorene reported by Pei *et al.* showed

unusually broad signals indicative of the insufficient purity or the isomer mixture of the sample. We have also encountered difficulty in the preparation and isolation of pure 2,2'-dibromo-9,9'-spirobifluorene by the direct dibromination of 9,9'-spirobifluorene. Alternatively, 2,2'-dibromo-9,9'-spirofluorene can be prepared by the replacement of amino group of 2,2'-diamino-9,9'-spirobifluorene by cupric bromide following conventional Sandmeyer procedure.[19] In addition to biphenyl-, azobenzene-, and phenol-type side products, Sandmeyer diazetization method are often plagued with position isomers of halide substituent.[22] In this case, 2,2'-dibromo-9,9'-spirobifluorene was obtained together with 2,3,2'-tribromo-9,9'-spirobifluorene and 2,2',3,3'-tetrbromo-9,9'- spirobifluorene as well, and the separation of these isomers remains difficult and greatly hampers materials applications. Therefore, pure 2,2'-dibromo-9,9'-spirobifluorene prepared in multigram scale is hard to come by and that greatly hampers materials applications. To prepare the starting material 2,2'-diamino-9,9'-spirobifluorene of the 2-donor-7-acceptor-9,9'-spirobifluorene become one of the most important issues in this research project.

Scheme 3-2

The synthesis of 2,7-dibromo-9,9'-spirobifluorene and 2,2'-dibromo-9,9'-spirofluorene

51
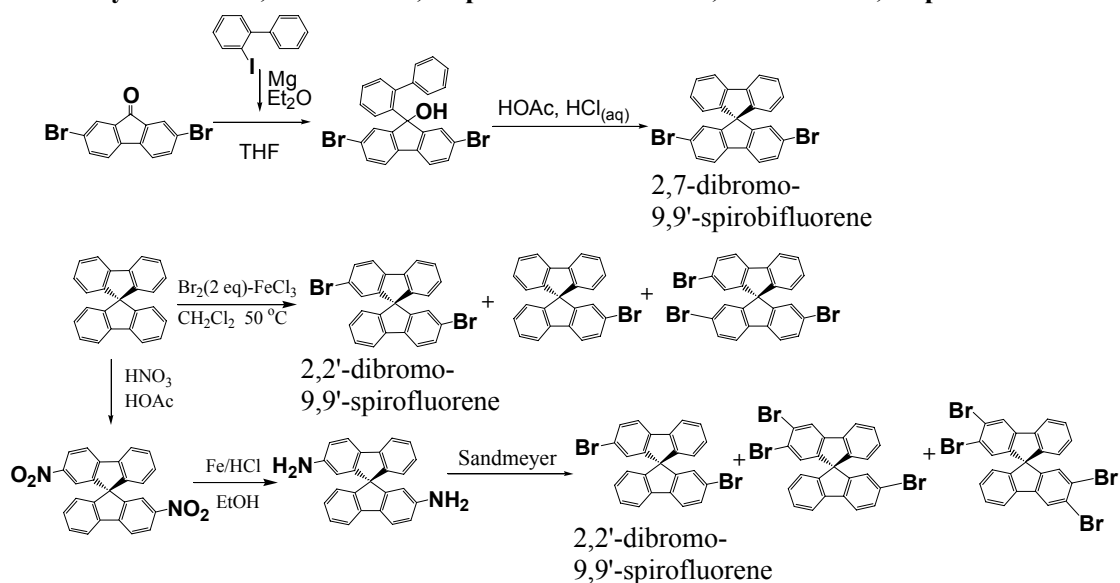
3-3 Experimental

3-3-1 Materials

The synthesis of **PhSPCHO** and **PhSPDCV** were descried in Chapter 2. 4-(Trimethylsily)phenylboronic acid, 2-(1,3-benzothiazol-2-yl)acetonitrile and diethoxy-diphenylmethylphosphonate were synthesized according to literature procedures. 1,2-Dibromobenzene 98%, tetrakis(triphenylphosphine)palladium(0), methyl carbonate, anhydrous sodium acetate, bromine, triethylamine, sodium sulfite, methanesulfonic acid, dichloromethyl methyl ether 98% (CH_3OCHCl_2), sodium bicarbonate, 2,2'-methylenebisbenzothiazole, sodium carbonate, Titanium tetrachloride ($TiCl_4$), sodium hydride 60% dispersion in mineral oil (NaH), diphenylamine, palladium(II) aetate ($Pd(OAc)_2$) with 47.5% palladium, tri-*tert*-butylphosphine 99% ($P(^tBu)_3$), cesium carbonate (Cs_2CO_3), malononitrile, basic aluminum oxide (Al_2O_3), *n*-butyllithium (n-BuLi) 1.6 M in hexane, *N,N'*-dimethylformamide (DMF), tetrahydrofuran (THF), calcium hydride, benzophenone, toluene, dichloromethane, ethyl acetate and hexane were purchased from Acros, Fluka, Aldrich, Riedel-dehaën, TCI, Merck or Mallunckrodt. DMF was distilled by calcium sulfate under reduced pressure. Toluene was distilled under nitrogen from calcium hydride. THF was distilled under nitrogen from sodium benzophenone ketyl, and the other solvents of were dried using standard procedures. All other reagents were used as received from commercial sources unless otherwise stated.

3-3-2 Instrument

All of the measurement methods of instruments were similar to the description of 2-3-1 in Chapter 2.

Theoretical Calculation: For theoretical dipole moment (μ) calculation, donor-acceptor-substituted spirobifluorene molecules were optimized with density functional theory

(DFT) with the hybrid B3LYP functional[23] and 6-31G* basis set. With the optimized structure, we have calculated the ground state dipole moments with the Hartree–Fock (HF) and the DFT (B3LYP) models and 6-31G* basis set. For all calculations, a developmental version of Q-Chem was used.[24] Excited state dipole moments were calculated using Configuration Interaction Singles (CIS)/6-31G*. In all cases the first excited states are highly optically active, as indicated by large oscillator strengths (> 0.9). Therefore we use the first CIS excited state to model the observed light-emitting states. We avoided using time-dependent DFT due to its problem in describing states with charge-transfer (CT) nature,[25] which may arise from the donor-acceptor moieties and such CT states might interfere with the optically active states we studied. Even though the CIS results might be less accurate than TDDFT, the qualitative trends in CIS results can still offer correct physical insights.

3-3-3 Synthesis
Synthesis of (2'-bromobiphenyl-4-yl)trimethylsilane (3-2)
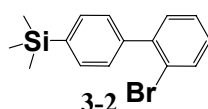
Under nitrogen atmosphere, a solution of 2 M Na_2CO_3 (80 mL) was added to the mixture of 4-(trimethylsily)phenylboronic acid **3-1** (15 g, 77.28 mmol), 1,2-dibromobenzene (21.9 g, 11.2 mL, 92.74 mmol), and tetrakis(triphenylphosphine) palladium(0) (1.1 g, 0.93 mmol) in toluene (160 mL). Then the mixture was refluxed with stirring for 24 h. After cooling to room temperature, saturated ammonium chloride solution was added to the reaction solution. The solution was extracted with ethyl acetate, dried over $MgSO_4$ and concentrated under reduced pressure. The solution was subjected to flash column chromatography (silica gel, hexane) to give colorless liquid. The product was farther purified by Kugelrohr vacuum distillation (0.4 torr, 145~152 °C). Yield: 76.3% (18 g). ^{1}H NMR (400 MHz, CDCl$_3$): δ

(ppm) 7.65 (dd, 1H, J = 8.0 Hz, 1.0 Hz), 7.57 (d, 2H, J = 8.0 Hz), 7.39 (d, 2H, J = 8.0 Hz), 7.29-7.37 (m, 2H), 7.15–7.22 (m, 1H), 0.30 (s, 9H). ^{13}C NMR (100 MHz, CDCl$_3$): δ (ppm) 142.5, 141.4, 139.7, 133.1, 133.0, 131.3, 128.7, 128.6, 127.4, 122.5, -1.1.   FAB-MS: calcd. 304.0, m/z = 289.1/291.1 (M-CH$_3^+$).

Synthesis of bis(4'-trimethylsilanylbiphenyl-2-yl)methanone (3-3)

3-3
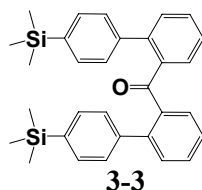
To a THF solution (100 mL) containing **3-2** (18 g, 59 mmol) was added n-BuLi (36.9 mL, 59 mmol, 1.6M in hexane) slowly at −78 °C.   The mixture was stirred for 2 h under nitrogen atmosphere.   After the slow addition of methyl carbonate (2.66 g, 29.5 mmol) THF solution (30 mL), the reaction solution was gradually warmed up to −45~−40 °C and kept at this temperature for 3 h to give yellow slurry.   The reaction mixture was then warmed to room temperature and stirred overnight.   Saturated ammonium chloride solution was added to the reaction solution.   The solution was extracted with ethyl acetate, dried over MgSO$_4$, and concentrated under reduced pressure.   The residue solid was subjected to flash column chromatography (silica gel, hexane) to give viscous oil.   The desired product was isolated by Kugelrohr vacuum distillation (0.4 torr, 175~180 °C).   Yield: 57.0% (8.0 g). ^{1}H NMR (400 MHz, CDCl$_3$): δ (ppm) 7.39 (d, 2H, J = 7.6 Hz), 7.31 (d, 4H, J = 7.4 Hz), 7.28 (t, 2H, J = 7.5 Hz), 7.13 (t, 2H, J = 7.6 Hz), 7.11 (d, 2H, J = 7.6 Hz), 7.07 (d, 4H, J = 7.4 Hz), 0.22 (s, 18H). ^{13}C NMR (100 MHz, CDCl$_3$): δ (ppm) 200.5, 141.5, 140.7, 139.2, 138.9, 132.8, 130.7, 130.5, 130.1, 128.2, 126.6, -1.2.   FAB-MS: calcd. 478.2, m/z = 479.1 (M+H$^+$).   Anal. Found (calcd.) for C$_{31}$H$_{34}$OSi$_2$: C 77.77 (77.77), H 7.36 (7.16).

Synthesis of bis(4'-bromobiphenyl-2-yl)methanone (3-4)

3-4
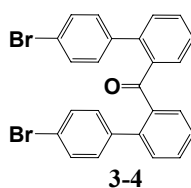
Under nitrogen atmosphere, a mixture of anhydrous sodium acetate (2.06 g, 25.08 mmol) and **3-3** (6 g, 12.54 mmol) in dry THF (100 mL) were cooled to 0 °C. Bromine (2.71 mL, 52.68 mmol) was added and the mixture was stirred at 0 °C for 12 h. The reaction solution was quenched by the addition of triethylamine (14.7 mL, 105.4 mmol), followed by an excess amount of aqueous Na_2CO_3. The product was extracted into diethyl ether, and the ether extract was washed with sodium sulfite solution and dried over $MgSO_4$ and concentrated under reduced pressure. The residue solid was subjected to flash column chromatography (silica gel, ethyl acetate/hexanes: 1/15). A white solid was obtained. Yield: 83.4% (6.1 g). ^{1}H NMR (400 MHz, CDCl$_3$): δ (ppm) 7.40 (d, 2H, J = 7.6 Hz), 7.38 (t, 2H, J = 7.6 Hz), 7.31 (d, 4H, J = 8.4Hz), 7.25 (t, 2H, J = 7.6 Hz), 7.13 (d, 2H, J = 7.6 Hz), 6.95 (d, 4H, J = 8.4 Hz). ^{13}C NMR (100 MHz, CDCl$_3$): δ (ppm) 199.5, 140.5, 139.3, 138.9, 131.04, 130.99, 130.7, 130.5, 130.2, 127.1, 121.6. FAB-MS: calcd. 489.9, m/z = 490.9/492.9/494.9 (M+H$^+$). Anal. Found (calcd.) for $C_{25}H_{16}Br_2O$: C 61.68 (61.00), H 4.09 (3.28).

**Synthesis of 2,2'-dibromo-9,9'-spirobifluorene (3-5)**

3-5
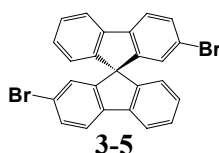
The **3-4** (6 g, 12.2 mmol) was added to methanesulfonic acid (200 mL) and stirred vigorously. The solution mixture was heated at 120 °C for overnight. After cooling to room temperature, the suspended solid was filtrated, and washed with water. The residue was subjected to flash column chromatography (silica gel, dichloromethane/ hexanes: 1/10).

A white solid was obtained. Yield: 77.4% (4.6 g). ^{1}H NMR (400 MHz, CDCl$_3$): δ (ppm) 7.79 (d, 2H, J = 7.6 Hz), 7.72 (d, 2H, J = 8.1 Hz), 7.49 (dd, 2H, J = 8.2 Hz, 1.8 Hz), 7.37 (td, 2H, J = 7.6 Hz, 1.1 Hz), 7.13 (td, 2H, J = 7.6 Hz, 1.1 Hz), 6.82 (d, 2H, J = 1.8 Hz), 6.70 (d, 2H, J = 7.6 Hz). ^{13}C NMR (100 MHz, CDCl$_3$): δ (ppm) 149.9, 147.7, 140.7, 140.6, 131.2, 128.4, 128.2, 127.3, 124.1, 121.5, 121.4, 120.2, 65.6.   FAB-MS: calcd. 471.9, m/z = 471.8/473.8/475.8 (M $^+$).   Anal. Found (calcd.) for C$_{25}$H$_{14}$Br$_2$: C 63.60 (63.32), H 3.21 (2.98).

Synthesis of 2,2'-dibromo-9,9'-spirobifluorene-7,7'-dicarboxaldehyde (BisBrSPCHO, 3-6)

BisBrSPCHO, 3-6
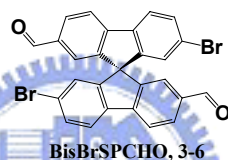
Under nitrogen atmosphere, 3-**5** (4.3 g, 9.07 mmol) was dissolved in CH$_2$Cl$_2$ (150 mL) at 0 ^{o}C.   A solution of TiCl$_4$ (24 mL, 219 mmol) in CH$_2$Cl$_2$ (30 mL) were added dropwise in 30 minutes with sufficient stirring.   The purple reaction mixture was stirred an addition 1 hour at 0 ^{o}C.   Then, the dilution of CH$_3$OCHCl$_2$ (6 mL, 66 mmol) in 30 mL of CH$_2$Cl$_2$ were added by dropping funnel over 30 minutes at 0 ^{o}C.   The dark green mixture was slowly allowed to reach room temperature and the mixture was stirred for additional 24 h.   The dark green mixture was added to crushed ice, the organic layer was separated and the aqueous layer was extracted with CH$_2$Cl$_2$.   The combined organic fractions were washed consecutively with saturated sodium bicarbonate, water, and finally dried over MgSO$_4$.   The solution was concentrated under reduced pressure, and subjected to flash column chromatography (silica gel, ethyl acetate/hexanes: 1/5).   A greenish yellow solid was obtained. Yield: 83.2% (4.0 g). ^{1}H NMR (400 MHz, CDCl$_3$): δ (ppm) 9.83 (s, 2H), 7.98 (d, 2H, J = 7.8 Hz), 7.92 (dd, 2H, J = 7.9 Hz, 1.3 Hz), 7.79 (d, 2H, J = 8.2 Hz), 7.58 (dd, 2H, J =

8.2 Hz, 1.7 Hz), 7.21 (s, 2H), 6.87 (d, 2H, J = 1.7 Hz).   ^{13}C NMR (100 MHz, CDCl$_3$): δ

(ppm) 191.2, 150.0, 147.6, 146.6, 139.2, 136.5, 132.1, 131.6, 121.5, 124.4, 123.7, 122.8,

120.8, 65.1.   FAB-MS: calcd. 527.9, m/z = 528.8/530.8/532.8 (M+H$^+$).   Anal. Found (calcd.)

for C$_{27}$H$_{14}$Br$_2$O$_2$: C 60.52 (61.16), H 2.75 (2.66).

**Synthesis of 2,2'-bis(diphenylamino)-9,9'-spirobifluorene-7,7'-dicarboxaldehyde (BisPhSPCHO, 3-7)**

BisPhSPCHO, 3-7
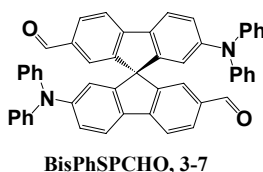
Under nitrogen atmosphere, a mixture of **3-6** (3.30 g, 6.22 mmol), diphenylamine (2.53

g, 14.94 mmol), Pd(OAc)$_2$ (69.9 mg, 0.31 mmol), Cs$_2$CO$_3$ (7.08 g, 21.73 mmol) and P(^{t}Bu)$_3$

(0.154 mL, 0.622 mmol) in toluene (45 mL) was heated at 120 ^{o}C with stirring overnight.

After cooling to room temperature, saturated ammonium chloride solution was added to the

reaction solution.   The solution was extracted with ethyl acetate, dried over MgSO$_4$.   The

solution was concentrated under reduced pressure and subjected to flash column

chromatography (silica gel, ethyl acetate/hexanes: 1/5).   A greenish yellow solid was

obtained.   Yield: 79.6% (3.5 g).   ^{1}H NMR (400 MHz, CDCl$_3$): δ (ppm) 9.82 (s, 1H), 7.81

(dd, 2H, J = 7.9 Hz, 1.4 Hz), 7.77 (d, 2H, J = 7.9 Hz), 7.65 (d, 2H, J = 8.4 Hz), 7.22 (d, 2H, J

= 1.4 Hz), 7.18 (t, 8H, J = 7.8 Hz), 6.91–7.03 (m, 14H), 6.58 (d, 2H, J = 2.0 Hz).   ^{13}C NMR

(100 MHz, CDCl$_3$): δ (ppm) 191.6, 150.4, 149.4, 148.6, 147.8, 147.2, 135.2, 134.5, 131.7,

129.2, 124.4, 123.9, 123.8, 123.3, 122.3, 119.8, 118.4, 65.2.   FAB-MS: calcd. 706.3, m/z =

706.0 (M$^+$).   Anal. Found (calcd.) for C$_{51}$H$_{34}$N$_2$O$_2$: C 85.83 (86.66), H 5.03 (4.85), N 3.37

(3.96).

Synthesis of 2,2'-bis(diphenylamino)-9,9'-spirobifluorene (BisPhSP, 3-8)

BisPhSP, 3-8
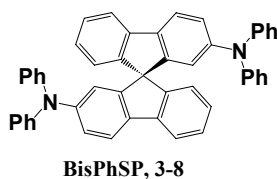
Under nitrogen atmosphere, a mixture of **3-5** (0.7 g, 1.48 mmol), diphenylamine (0.76 g, 4.44 mmol), Pd(OAc)$_2$ (18 mg, 0.082 mmol), Cs$_2$CO$_3$ (1.74 g, 5.33 mmol) and P(^{t}Bu)$_3$ (0.038 mL, 0.15 mmol) in toluene (10 mL) was heated at 120 ^{o}C with stirring overnight.   After cooling to room temperature, saturated ammonium chloride solution was added to the reaction solution.   The solution was extracted with ethyl acetate, dried over MgSO$_4$.   The solution was concentrated under reduced pressure and subjected to flash column chromatography (silica gel, ethyl acetate/hexanes: 1/10).   A white solid was obtained.   Yield: 82.9% (0.8 g). ^{1}H NMR (400 MHz, CDCl$_3$): δ (ppm) 7.65 (d, 2H, J = 7.6 Hz), 7.59 (d, 2H, J = 8.2 Hz), 7.28 (td, 2H, J = 7.5 Hz, 1.0 Hz), 7.15 (t, 8H, J = 7.4 Hz), 7.04 (td, 2H, J = 7.5 Hz, 1.0 Hz), 6.88-6.99 (m, 7H), 6.72 (d, 2H, J = 7.5 Hz), 6.64 (d, 2H, J = 1.9 Hz). ^{13}C NMR (100 MHz, CDCl$_3$): δ (ppm) 150.0, 148.8, 147.7, 147.4, 141.3, 136.9, 129.1, 127.6, 127.0, 124.5, 123.73, 123.65, 122.5, 120.7, 120.0, 119.4, 66.8.   FAB-MS: calcd. 650.3, m/z = 650.0 (M$^+$).   Anal. Found (calcd.) for C$_{49}$H$_{34}$N$_2$: C 90.22 (90.43), H 5.58 (5.27), N 4.25 (4.30).

**Synthesis of 2,2'-bis(diphenylamino)-7,7'-bis(2,2-diphenylvinyl)-9,9'- spirobifluorene (BisPhSPDPV, 3-9)**

BisPhSPDPV, 3-9
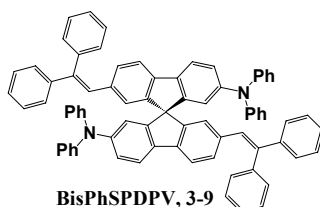
Under nitrogen atmosphere, to diethoxydiphenylmethylphosphonate (1.0 g, 3.2 mmol) in dry THF (10 mL) was added NaH (0.13 g, 60 wt% in oil, 3.3 mmol), and stirred for 1 hr at 55 ^{o}C. Cooling to room temperature, **3-7** (0.2 g, 0.28 mmol) was added, the reaction solution

was heated at reflux temperature overnight. After cooling to temperature, the reaction mixture was added to water, extracted with ethyl acetate, dried over MgSO$_4$. The solution was concentrated under reduced pressure and subjected to flash column chromatography (silica gel, dichloromethane/hexanes: 1/2). A greenish blue solid was obtained. Yield: 87.0% (0.25 g). ^{1}H NMR (400 MHz, CDCl$_3$): δ (ppm) 7.46 (d, 2H, J = 8.2 Hz), 7.35 (d, 2H, J = 8.0 Hz), 7.20–7.32 (m, 10H), 7.10–7.20 (m, 14H), 7.04–7.10 (m, 4H), 6.90–7.02 (m, 10H), 6.87 (s, 2H), 6.55 (d, 2H, J = 2.0 Hz), 6.19 (d, 2H, J = 1.3 Hz). ^{13}C NMR (100 MHz, CDCl$_3$): δ (ppm) 150.1, 148.5, 147.7, 147.3, 143.2, 141.7, 140.3, 139.9, 136.1, 129.8, 129.3, 129.1, 128.6, 128.3, 128.2, 127.4, 127.3, 124.6, 124.3, 123.7, 122.5, 120.7, 119.9, 118.8, 65.3. FAB-MS: calcd. 1006.4, m/z = 1006.3 (M$^+$). Anal. Found (calcd.) for C$_{77}$H$_{54}$N$_2$: C 91.0 (91.82), H 5.33 (5.40), N 2.73 (2.78).

Synthersis of 7,7'-bis(2,2-bis(benzothiazol-2-yl)vinyl)-2,2'-bis(diphenylamino)-9,9'-spirobifluorene (BisPhSPDBTV, 3-10)

BisPhSPDBTV, 3-10
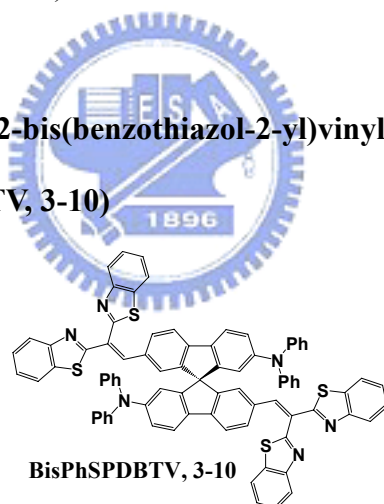
3-7 (0.8 g, 1.13 mmol), 2,2'-methylenebisbenzothiazole (0.93 g, 3.18 mmol, 97%), and basic aluminum oxide (1.5 g) are stirred in toluene (20 mL) for 48 h at reflux temperature. After cooling to room temperature, the reaction solution was filtered. The filtrate was subjected to flash column chromatography (silica gel, dichloromethane/hexanes: 1/1). A red solid was obtained. Yield: 50.9% (0.8 g). ^{1}H NMR (400 MHz, CDCl$_3$): δ (ppm) 8.03 (s, 2H), 7.99 (d, 2H, J = 8.2 Hz), 7.96 (d, 2H, J = 8.2 Hz), 7.77 (d, 2H, J = 7.8 Hz), 7.75 (d, 2H, J = 7.9 Hz), 7.49 (t, 2H, J = 8.2 Hz), 7.41 (t, 4H, J = 7.9 Hz), 7.30 (d, 2H, J = 7.5 Hz), 7.11–7.25 (m, 12H), 7.08 (dd, 2H, J = 8.1 Hz, 1.1 Hz), 6.86-7.00 (m, 12H), 6.82 (dd, 2H, J =

8.3 Hz, 2.0 Hz), 6.47 (d, 2H, J = 1.9 Hz), 6.32 (s, 2H). ^{13}C NMR (100 MHz, CDCl$_3$): δ (ppm) 167.5, 164.1, 153.6, 153.1, 149.5, 148.3, 148.1, 147.4, 142.3, 138.4, 136.1, 135.4, 135.3, 132.3, 131.1, 126.5, 126.3, 126.1, 125.6, 125.0, 124.7, 124.1, 124.0, 123.8, 123.1, 122.8, 122.4, 122.1, 121.3, 121.3, 65.0. FAB-MS: calcd. 1234.3, m/z = 1235.0 (M+H$^+$). Anal. Found (calcd.) for C$_{81}$H$_{50}$N$_6$S$_4$: C 78.43 (78.74), H 4.10 (4.08), N 7.02 (6.80).

**Synthesis of 7,7'-bis(2-benzothiazol-2-yl-2-cyanovinyl)-2,2'-bis(diphenylamino)-9,9'-spirobifluorene (BisPhSPCNBTV, 3-11)**
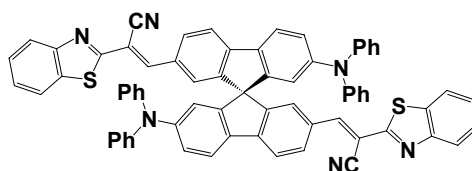

BisPhSPCNBTV, 3-11

3-7 (0.9 g, 1.27 mmol), 2-(1,3-benzothiazol-2-yl)acetonitrile (0.56 g, 3.2 mmol), and basic aluminum oxide (1.5 g) are stirred in toluene (20 mL) for 24 h at 100 ^{o}C. After cooling to room temperature, the reaction solution was filtered. The filtrate was subjected to flash column chromatography (silica gel, dichloromethane/hexanes: 1/1). A red solid was obtained. The minor *cis*-isomer can be all converted to *trans*-isomer in chloroform under the radiation of long wavelength UV light (365 nm). Yield: 69.4% (0.9 g). ^{1}H NMR (400 MHz, CDCl$_3$): δ (ppm) 8.25 (dd, 2H, J = 8.2 Hz, 1.6 Hz), 8.07 (s, 2H), 7.98 (d, 2H, 8.1 Hz), 7.84 (d, 2H, J = 7.8 Hz), 7.79 (d, 2H, J = 8.2 Hz), 7.67 (d, 2H, J = 8.4 Hz), 7.47 (td, 2H, J = 8.4 Hz, 1.2 Hz), 7.37 (td, 2H, J = 8.2 Hz, 1.1 Hz), 7.19 (t, 8H, J = 7.4 Hz), 7.14 (d, 2H, 1.5 Hz), 6.95–7.05 (m, 14H), 6.65 (d, 2H, 2.0 Hz). ^{13}C NMR (100 MHz, CDCl$_3$): δ (ppm) 163.0, 153.6, 150.0, 149.3, 148.8, 147.3, 146.6, 145.6, 134.9, 134.7, 130.9, 129.5, 129.2, 126.9, 126.8, 125.7, 124.4, 123.9, 123.34, 123.30, 122.1 121.6, 120.3, 118.5, 116.7, 103.7, 65.4. FAB-MS: calcd. 1018.3, m/z = 1019.1 (M+H$^+$). Anal. Found (calcd.) for C$_{69}$H$_{42}$N$_6$S$_2$: C 80.79 (81.31), H 4.47 (4.15), N 7.66 (8.25).

Synthersis of 7,7'-bis(2,2-dicyanovinyl)-2,2'-bis(diphenylamino)-9,9'-spirobifluorene (BisPhSPDCV, 3-12)

BisPhSPDCV, 3-12
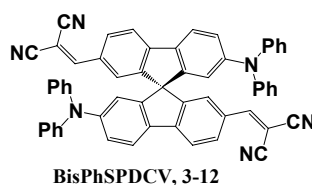
3-7 (2.1 g, 2.97 mmol), malononitrile (0.8 g, 12.11 mmol), and basic aluminum oxide (4.0 g) are stirred in toluene (25 mL) for 24 h at 100 ^{o}C. After cooling to room temperature, the reaction solution was filtered. The filtrate was subjected to flash column chromatography (silica gel, ethyl acetate/hexanes: 1/5). A red solid was obtained. Yield: 67.1% (1.6 g). ^{1}H NMR (400 MHz, CDCl$_3$): δ (ppm) 7.95 (dd, 2H, J = 8.1 Hz, 1.6 Hz), 7.75 (d, 2H, J = 8.1 Hz), 7.66 (d, 2H, J = 8.4 Hz), 7.54 (s, 1H), 7.20 (t, 8H, J = 7.8 Hz), 7.08 (d, 2H, J = 1.6 Hz), 7.05–6.95 (m, 14H), 6.58 (d, 2H, J = 2.0 Hz). ^{13}C NMR (100 MHz, CDCl$_3$): δ (ppm) 159.0, 150.1 149.9, 148.7, 148.0, 147.0, 133.6, 131.1, 129.3, 126.0, 124.6, 123.8, 123.7, 122.7, 120.4, 117.7, 114.1, 112.9, 80.3, 65.1. FAB-MS: calcd. 802.3, m/z = 802.1 (M^{+}). Anal. Found (calcd.) for C$_{57}$H$_{34}$N$_6$: C 85.26 (85.44), H 4.27 (4.22), N 10.47 (10.37).

Synthersis of 2-diphenylamino-7-2,2'-diphenylvinyl-9,9'-spirobifluorene (PhSPDPV, 3-13)

PhSPDPV, 3-13
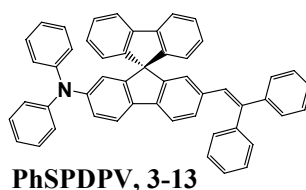
Under nitrogen atmosphere, to diethoxydiphenylmethylphosphonate (1.88 g, 6.02 mmol) in dry THF (10 mL) was added NaH (0.26 g, 60 wt% in oil, 6.20 mmol), and stirred for 1 hr at 55 ^{o}C. Cooling to room temperature, 2-diphenylamino-9,9'-spirobifluorene-7-dicarboxaldehyde (1.50 g, 2.93 mmol) was added, the reaction solution was heated at reflux temperature overnight. After cooling to temperature, the reaction mixture was added to

water, extracted with ethyl acetate, dried over MgSO$_4$.   The solution was concentrated under reduced pressure and subjected to flash column chromatography (silica gel, dichloromethane/hexanes: 1/5).   A greenish blue solid was obtained.   Yield: 87.6% (1.7 g). ^{1}H NMR (400 MHz, CDCl$_3$): δ (ppm) 7.66 (d, 2H, J = 7.6 Hz), 7.57 (d, 1H, J = 8.3 Hz), 7.49 (d, 1H, J = 8.0 Hz), 7.29 (td, 2H, J = 7.5 Hz, J = 0.9 Hz), 7.17–7.22 (m, 5H), 6.97-7.11 (m, 10H), 6.92–6.97 (m, 3H), 6.85–6.97 (m, 6H), 6.78 (s, 1H), 6.71 (d, 1H, J = 7.6 Hz), 6.48 (d, 1H, J = 2.0 Hz), 6.11 (s, 1H). ^{13}C NMR (125 MHz, CDCl$_3$): δ (ppm) 150.3, 148.6, 148.4, 147.5, 147.4, 143.2, 141.9, 141.5, 140.0, 139.9, 136.5, 136.2, 129.8, 129.4, 129.0, 128.3, 128.1, 127.5, 127.4, 127.3, 127.2, 124.8, 124.0, 123.8, 122.5, 120.5, 119.9, 118.8, 65.6. FAB-MS: calcd. 661.8, m/z = 661.3 (M$^+$).   Anal. Found (calcd.) for C$_{51}$H$_{35}$N: C 92.35 (92.55), H 5.49 (5.33), N 2.49 (2.12).
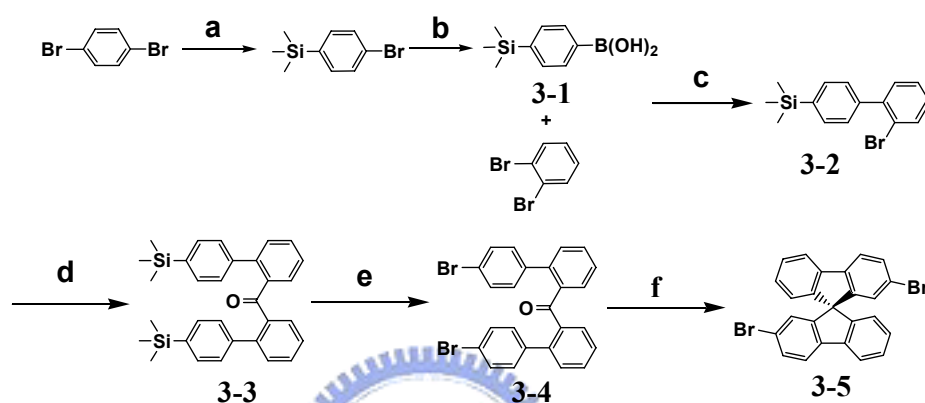
3-4 Results and Discussion

3-4-1 Improved synthesis of 2,2'-dibromo-9,9'-spirobifluorene and its 2,2'-bisdonor-7,7'-bisacceptor-substituted -9,9'-spirobifluorene derivatives.

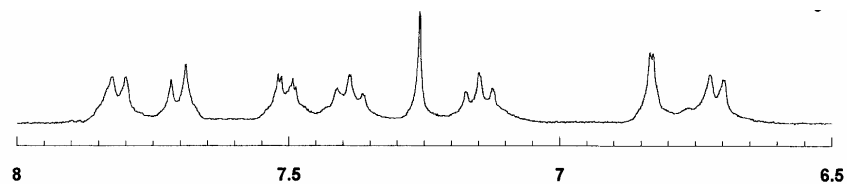#### 3-4-1-1 Synthesis of 2,2'-dibromo-9,9'-spirobifluorene

Scheme 3-3

Reagents and conditions: (a) n-BuLi, THF, −78 ^{o}C, then trimethylsilanyl chloride in THF, RT, overnight, 82%; (b) n-BuLi, THF, −78 ^{o}C, then trimethoxybroane, RT, overnight, 95%; (c) Pd(PPh$_3$)$_4$, 2 M Na$_2$CO$_{3(aq)}$, toluene, 120 ^{o}C, 24 h, 76%; (d) n-BuLi, THF, −78 ^{o}C, 2 h, then methyl carbonate in THF, −40 ^{o}C, 3 h, then, RT, overnight, 57%; (e) NaOAc/Br$_2$, THF, 0 ^{o}C, then Et$_3$N, 0 ^{o}C, 83%; (f) CH$_3$SO$_3$H, 120 ^{o}C, overnight, 77%.

A new method to prepare 2,2'-dibromo-9,9'-spirobifluorene in multigram scale was developed in Scheme 3-3. The key starting material in the preparation of 2,2'-dibromo-9,9'-spirobifluorene is 4-(trimethylsilyl) benzeneboronic acid, which is commercially available. It can be also readily prepared in a two-step reaction from 1,4-bibromobenzene and chlorotrimethylsilane followed by the treatment of *n*-BuLi and trimethylborate in formation of boronic acid. More than 30 grams of 4-(trimethylsilyl)-benzeneboronic acid can be prepared easily in totally overall yields of 75% by following the report of literature.[25] The desired 2,2'-dibromo-9,9'-spirobifluorene was prepared in 4 steps from 4-(trimethylsilyl)benzeneboronic acid (**3-1**) in total overall yields near 30%.

Suzuki coupling of **3-1** with equivalent 1,2- dibromobenzene under standard condition yielded (2'-bromobiphenyl-4-yl)trimethylsilane (**3-2**) in 76%.   The next step of the synthesis led to the ketone- connected dimer of (2'-bromobiphenyl-4-yl)trimethylsilane (**3-3**) that was treated with *n*-BuLi and reacted with 0.5 equivalent of dimethylcarbonate in 57%.[26]   The following bromodesilation of the disilane compound by sodium acetate and bromine easily afforded bis-(4'-bromobiphenyl-2-yl)methanone (**3-4**) in 83%.   The target product was thus obtained by classical Clark and Gomberg method in the present of strong acid of methanesulfonic acid.[27]   Compare to the ^{1}H NMR spectrum of 2,2'-dibromo-9,9'-spirobifluorene reported by Pei *et al.* using the direct bromination of 9,9'-spirobifluorene showed in **Figure 3-6(a)**,[6c] unusually broad signals indicative of the insufficient purity or the isomer mixture of the sample.   The 2,2'-dibromo-9,9'- spirobifluorene (**3-5**) compound prepared by the new method was pure and efficient (**Figure 3-6(b)**).   The X-ray single crystal structure was showed in **Figure 3-6(c)**.   Multi-gram quantity of 2,2'-dibromo-9,9'-spirobifluorene can be prepared readily (here 4.6 g of the analytically pure product was obtained in one round).
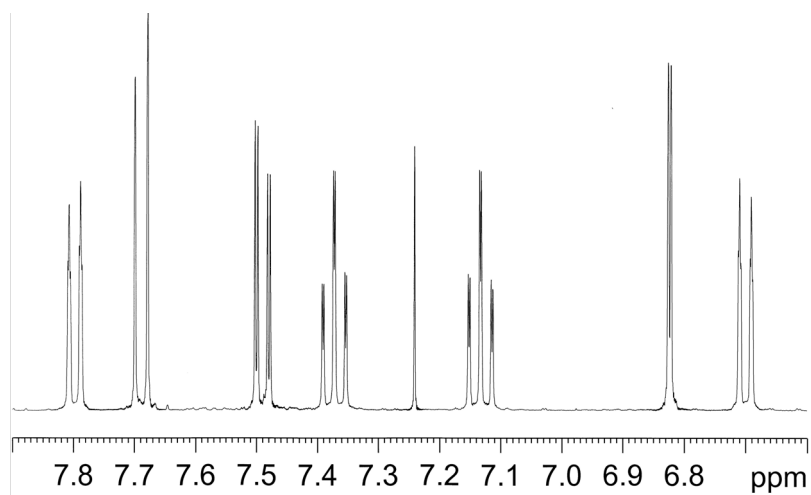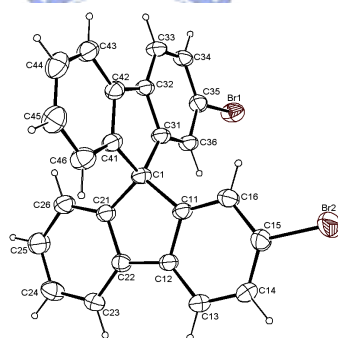
Figure 3-6. ^{1}H NMR (CDCl₃, 7.24 ppm) spectrum of 2,2'-dibromo-9,9'- spirobifluorene (a) The direct bromination of 9,9'-spirobifluorene by Pei *et al.* [6c] (b) This work. (c) Single crystal X-ray structure of 2,2'-dibromospirobifluorene.

3-4-1-2 Synthesis of 2,2'-bisdonor-7,7'-bisacceptor-substituted-9,9'- spirobifluorene derivatives

Scheme 3-4
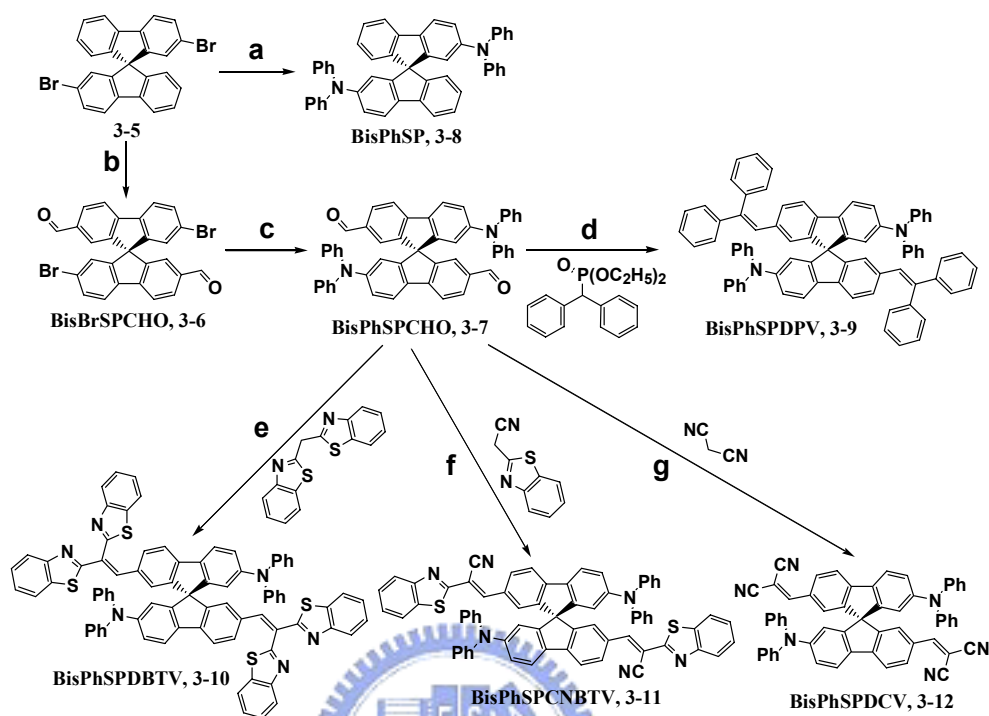
Reagents and conditions: (a) diphenylamine, Cs$_2$CO$_3$, Pd(OAc)$_2$, P(^{t}Bu)$_3$, toluene, 120 ^{o}C, overnight, 83%; (b) TiCl$_4$, CH$_2$Cl$_2$, then CH$_3$OCH$_2$Cl$_2$, 0 ^{o}C, overnight, 83%; (c) diphenylamine, Cs$_2$CO$_3$, Pd(OAc)$_2$, P(^{t}Bu)$_3$, toluene, 120 ^{o}C, overnight, 79%; (d) NaH, THF, 55 ^{o}C, overnight, 87%; (e) basic Al$_2$O$_3$, toluene, reflux, 48 h, 51%; (f) basic Al$_2$O$_3$, toluene, 100 ^{o}C, 24 h, 69%; (g) basic Al$_2$O$_3$, toluene, 100 ^{o}C, 24 h, 67%.

With a sufficient amount of pure 2,2'-dibromo-9,9'-spirobifluorene, we quickly prepared a series of new fluorescent 9,9'-spirobifluorene derivatives based on orthogonally constructed pair of donor-acceptor substituents (Scheme 3-4). **BisPhSP** was directly obtained from 2,2'-dibromo-9,9'-spirobifluorene by Pd- catalyzed aromatic amination reaction with a 83% yield. In order to develop a bis-type compare to **BrSPCHO** in Charpter 2, two formyl functional groups were need added to 7 and 7' positions of 2,2'-dibromo-9,9'-spirobifluorene. 2,2'-dibromo-7,7'-diformyl-9,9'-spirobifluorene (**BisBrSPCHO**, **3-6**), which was easily prepared by the one-step di-formylation of 2,2'-dibromo-9,9'-spirobifluorene carried on using CH$_3$OCHCl$_2$/TiCl$_4$ with a 83% yield.[27]

BisPhSPCHO was synthesized from 2,2'- dibromo-7,7'-diformyl-9,9'-spirobifluorene by the same synthetic condition of **BisPhSP**.   Using aldehyde **BisPhSPCHO** as the common starting material, various acceptor bisbenzothiazolylvinyl-, benzothiazolylcyanovinyl-, or dicyanovinyl- appended **BisPhSP**, *i.e.* **BisPhSPDBTV**, **BisPhSPCNBTV**, and **BisPhSPDCV** were smoothly generated in 51-69% yields under Knoevenagel conditions (basic Al_2O_3 in dry toluene).   For the synthesis of **BisPhSPDPV**, the efficient Horner−Wadsworth−Emmons reaction was conducted for the formation of the C-C double to connect **BisPhSPCHO** and diethoxydiphenylmethylphosphonate[28] with a 87% yield.

3-4-1-3   Optical   properties   of   2,2'-bisdonor-7,7'-bisacceptor-substituted-9,9'-spirobifluorene derivatives

The absorption bands arising from the π-π* and intramolecular charge-transfer transitions (ICT) were both observed **(Figure 3-7(a))**.   Specifically, ICT occurs as the lowest energy band in the spectra that can be attributed to the charge transfer from diarylamino donor to electron acceptors expect **BisPhSP** which only π-π* was observed.   Six new spirobifluorenes exhibited fluorescence with varied colors ranging from the deep blue (λ^{fl}_{max} of 401 nm) of **BisPhSP,** sky blue (λ^{fl}_{max} of 480 nm) of **BisPhSPDPV**, green blue of **BisPhSPCHO** (λ^{fl}_{max} of 495 nm), yellow orange (λ^{fl}_{max} of 549 nm) of **BisPhSPDBTV**, orange red (λ^{fl}_{max} of 601 nm) of **BisPhSPCNBTV**, to the vivid red (λ^{fl}_{max} of 620 nm) of **BisPhSPDCV** showed in **Figure 3-7(b)** and **(d)**.   Except of **BisPhSPDBTV**, all new bisdonor-bisacceptor- substituted 9,9'-spirobifluorene compounds showed pronounced fluorescence in solution (**Figure 3-7(d), (e)**).   When they were in the form of a solid film, red- shifting fluorescence generally took place.   Fluorescence with different brightness was observed for these fluorophores in solution as well in solid state (see **Figure 3-7(c)** and **(e)**).   Qualitatively, solid state fluorescence intensities (fluorescence quantum yields, Φ^{fl}s) in general follow the same order as those are solution (**Table 3-1**).   The strongest fluorescence

was found for **BisPhSPDPV** and **BisPhSPCHO**; **BisPhSP** and **BisPhSPDCV** showed second-rate fluorescence intense; weak fluorescence or no fluorescence was observed for **BisPhSPCNBTV** and **BisPhSPDBTV**, respectively.   Considering the strong fluorescence in solid state, some of the fluorophores in this report are worth further investigation for potential application of organic light-emitting diodes (OLEDs).
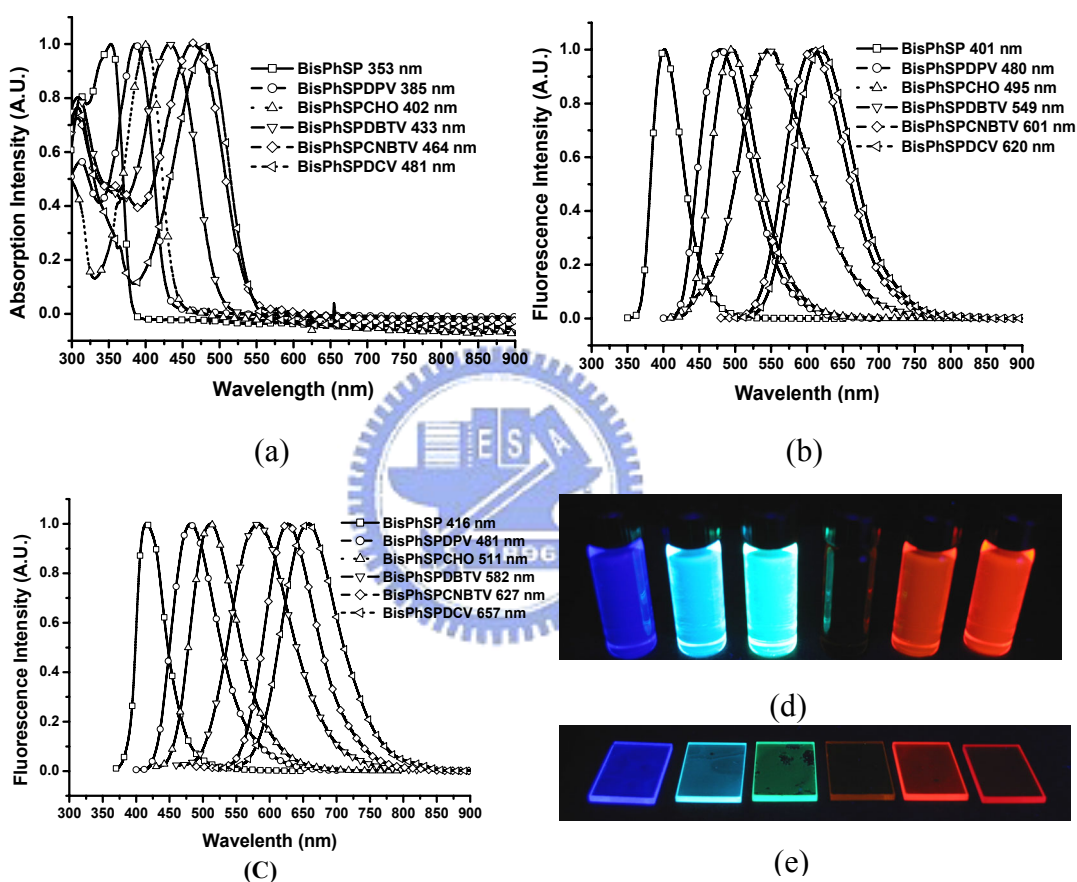
Figure 3-7. (a) Absorption spectra and (b) emission spectra of **BisPhSP, BisPhSPDPV**, **BisPhSPCHO, BisPhSPDBTV, BisPhSPCNBTV** and **BisPhSPDCV** in chlorobenzene, respectively. (c) Fluorescence spectra of 2,2'-bisdonor-7,7'-bisaccaptor-substituted 9,9'-spirobifluorenes in solid state (spin-coated solid films)   (d) Fluorescence images of the solution (in chlorobenzene). (e) Fluorescence images (spin-coated solid films).

Table 3-1. Fluorescence and absorption data of 2,2'-bisdonor-7,7'-bisaccaptor- substituted 9,9'spirobifluorenes.

	λ^{ab}_{max}, ε Clbenzene (nm, M^{-1}cm^{-1})	λ^{fl}_{max} Clbenzene (nm)	λ^{fl}_{max} Solid (nm)	Φ_f Clbenzene (%)
BisPhSP	353, 42300	401	416	24
BisPhSPDPV	385, 84700	480	481	50
BisPhSPCHO	402, 49700	495	511	46
BisPhSPDBTV	433, 59900	549	582	~0
BisPhSPCNBTV	464, 65800	601	627	14
BisPhSPDCV	481, 66200	620	657	31

3-4-1-4 Summary

In summary, we have successfully demonstrated that 2,2'-dibromo-9,9'- spirobifluorene can be prepared by a new method that does not go through the bromination or Sandmeyer reaction. Multi-grams of pure 2,2'-dibromo-9,9'- spirobifluorene can be readily obtained by the new synthetic method without the contamination of bromine-substituent position isomers. From 2,2'-dibromo-9,9'-spirobifluorene we have also synthesized six donor-acceptor-substituted 9,9'-spirobifluorene. These new 9,9'-spirobifluorene derivatives show varied fluorescence color and intensity of and they have potential for light-emitting application. We chose **BisPhSPDPV** vs **PhSPDPV** (synthesis not yet), **BisPhSPCHO** vs **PhSPCHO** and **BisPhSPDCV** vs **PhSPDCV** as the subjects of further investigation of emission optical and molecular dipole properties on photoluminescence and eelectroluminescence.

3-4-2 Characterization of BisPhSPDPV vs PhSPDPV, BisPhSPCHO vs PhSPCHO and BisPhSPDCV vs PhSPDCV

Scheme 3-5

PhSPDCV   PhSPCHO   PhSPDPV

BisPhSPDCV   BisPhSPCHO   BisPhSPDPV
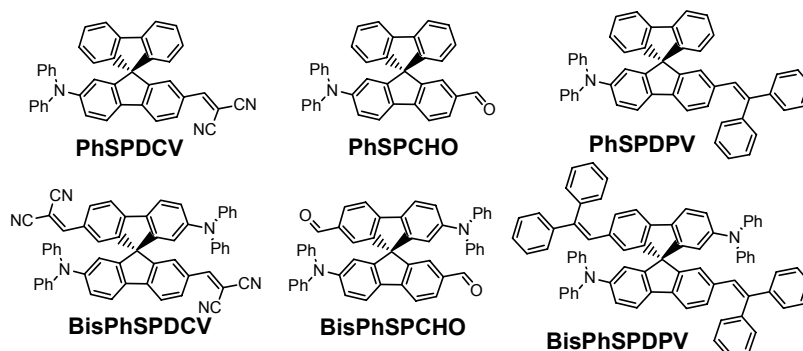
All the materials were collected in Scheme 3-5. The synthesis of **PhSPDCV** and **PhSPCHO** werer described in the section 2-3-1 of Chapter 2. The synthesis of **BisPhSPDCV**, **PhSPCHO** and **BisPhSPDPV** were described in the section 3-3-1-2 of this chapter. Only the **PhSPDPV** was lack for the description of synthesis, the **PhSPDPV** was adopted from the preparation of **BisPhSPDPV**. It was the efficient Horner-Wadsworth-Emmons reaction: reacting **PhSPCHO** with the yield of diethoxydiphenylmethylphosphonate that was generated in advance by sodium hydride in dry THF.

3-4-2-1 Thermal analysis

Except of **PhSPCHO**, all six spirobifluorene compounds are semi-amorphous materials because they were all detected for T_g but not T_c in differential scanning calorimetry (DSC) analysis **(Table 3-2)**. In general, the "dimeric" spirobifluorene compounds, (**BisPhSPDCV**, **BisPHSPCHO**, and **BisPhSPDPV**) have 16~23 ^{o}C higher T_gs than the corresponding "monomeric" spirobifluorene compounds (**PhSPDCV**, **PhSPCHO**, and **PhSPDPV**) because of higher molecular weight. A similar trend was found for the thermal stability property (T_ds) of six compounds. The results suggested that they were all potential to form

morphologically stable thin film in solid state with limited crystallization.   This is one of the criteria that six spirobifluorene compounds meet the requirement of materials for non-dopant usage in OLEDs fabrication.

Table 3-2. Thermal properties of spirobifluorene compounds

	T_m (°C)	T_g (°C)	T_c (°C)	T_d (°C)
PhSPDCV	253	110	Not observed	337
BisPhSPDCV	266	133	Not observed	412
PhSPCHO	289	104	177	350
BisPhSPCHO	282	125	Not observed	387
PhSPDPV	223	112	Not observed	405
BisPhSPDPV	244	128	Not observed	442

All of T_ms only observed in the first heating scan.

3-4-2-2 Crystal X-ray Structure

BisPhSPDCV

Unlike the row-like loose molecular stacking of **PhSPDCV** in Chapter 2, a pair wise segregated molecular stacking was found in the crystal packing diagram of **BisPhSPDCV** (**Figure 3-8**).   The closest contact distance between molecules was found to be 3.38 Å, which is between C55 of dicyanovinyl acceptor and C40 of diphenylamino donor of the adjacent molecule.   This contact is potentially a π-π interaction and may devastate fluorescence in solid state.   However a careful examination of the crystal packing structure reveals that it is not a direct face to face π-π interaction but a side-way sliding and unparallel π-π contact between the dicyanovinyl C-C double bond and the phenyl ring of diphenylamino group (Figure 3-9.).   Although non-crystallinic amorphous phase is most likely to occur in the thin films of OLEDs, the information of the molecular packing in single crystal provides the worst scenario of possible molecular contact in thin film state.
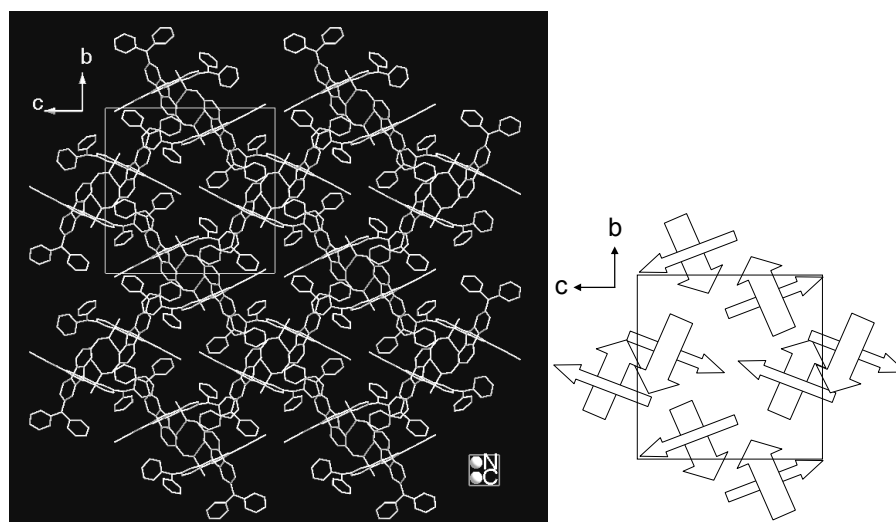
Figure 3-8. X-ray determined molecular structure and crystal packing diagram of **BisPhSPDCV**. The solvent molecules (toluene) solvated in the crystal packing were removed for clarity. The arrows in the cartoon of packing diagram at bottom right denote the direction from diphenylamino to dicyanovinyl substituent.
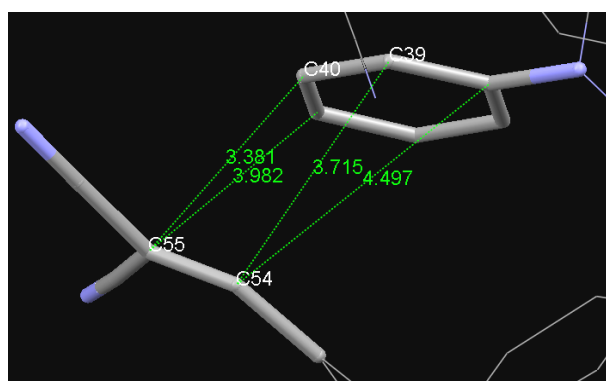
Figure 3-9. Close-up view of the interaction between **BisPhSPDCV** molecules. The figure reveals the side-way sliding and unparallel position of dicyanovinyl and the phenyl ring of the diphenylamino group.

There is one thing interesting about the crystal structure of **BisPhSPDCV**. We obtained single crystal of **BisPhSPDCV** from several mix solvent systems, a mixture of

hexanes and chloroform/dichloromethane, toluene, 1,2-dichloroethane, or carbon tetrachloride. As far as X-ray diffraction concerns, these single crystals possess the same molecular packing of which different solvent molecules are solvated. Regardless different solvated molecules, all these single crystals had very similar crystal cell parameters. **Figure 3-10** illustrates two crystal packing diagrams of **BisPhSPDCV** single crystal and they are virtually identical, except that they contain different solvated molecules of toluene (left figure) and carbon tetrachloride (right figure). From this result it is conceivable that crystal packing exists with large void spaces occupied by the solvent molecules, which stabilize the packing structure. Such result implies that, under the condition of no solvated molecules (i.e., thermal vacuum deposition of OLED fabrication), **BisPhSPDCV** probably aggregate in a loose-contact form when the material is fabricated as a thin film material in OLEDs.
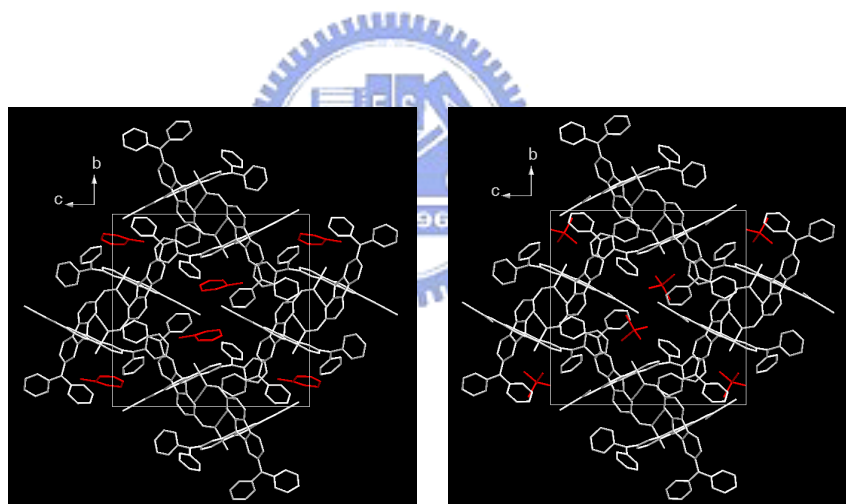
Figure 3-10. BisPhSPDCV crystal packing diagrams containing solvated molecules, toluene (left figure) and carbon tetrachloride (right figure). Solvated molecules are labeled in red color.

PhSPCHO and BisPhSPCHO

Different from the crystal of **BisPhSPDCV**, **PhSPCHO** and **BisPhSPCHO** crystallized without solvated solvent molecules (see **Figure 3-11** and **Figure 3-12**). There is no intermolecular face-on π-π interaction. The intermolecular contacts are either non-orthogonal edge-to-face (C-H···π) or unparallel face-to-face π-π interaction, such as a

73

3.34 Å contact distance between C19 and C45, which is in between two unparallel (~47°) π-conjugated six-member rings (**Figure 3-13**).   The closest contact found for the crystal of **PhSPCHO** is a 3.31 Å contact between C34-C35 double bond and that of adjacent molecule. This is a short distance contact but it is an edge-to-edge side way interaction between two phenyl rings of neighboring molecules (**Figure 3-14**), and it is unlikely to cause significant florescence quench.
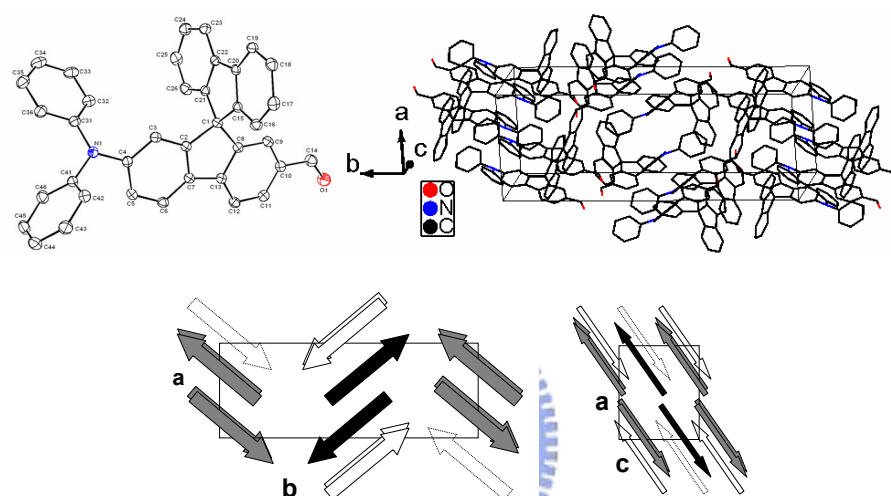
Figure 3-11. X-ray determined molecular structure and crystal packing diagram of **PhSPCHO**.   The arrows in the packing diagram at the bottom indicate the direction from diphenylamino to formyl substituent
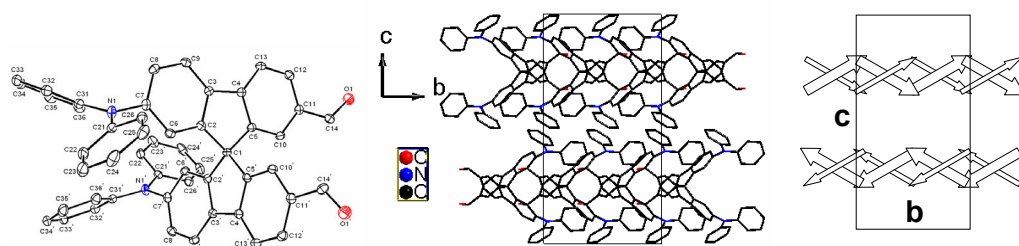
Figure 3-12. X-ray determined molecular structure and crystal packing diagram of **BisPhSPCHO**.   The arrows in the packing diagram at the bottom indicate the direction from the diphenylamino to formyl substituent
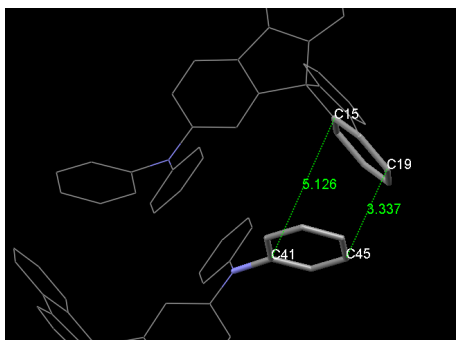
Figure 3-13. A unparallel ring-to-ring contact between C19 and C45 (3.34 Å) of **PhSPCHO**.
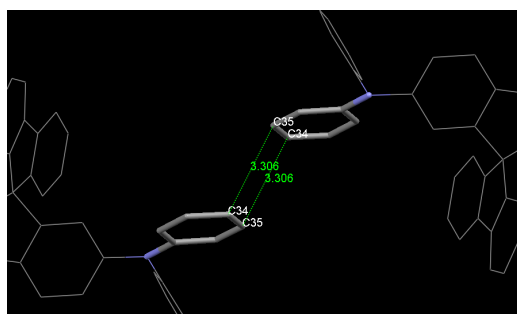
Figure 3-14. An edge-to-edge side way interaction between two phenyl rings of neighboring molecules of **PhSPCHO**.
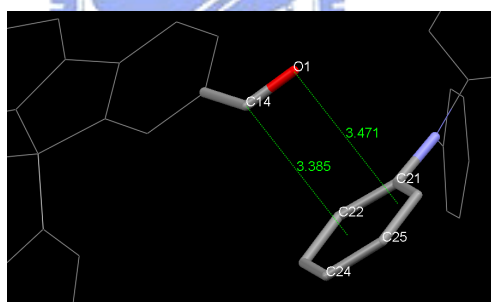
Figure 3-15. The face-on π-π interaction between formyl acceptor and the phenyl ring of diphenylamino donor of **BisPhSPCHO**.

For the crystal structure of **BisPhSPCHO**, a direct nearly face-on π-π interaction (~3.4 Å) was observed between phenyl ring of the diphenylamino donor and the C14-O1 double bond of the formyl acceptor of neighboring molecule (**Figure 3-15**). Furthermore, because of crystal packing symmetry, such face-on π-π interaction of **BisPhSPCHO** occurs twice for each molecule in the crystal. Therefore, more fluorescence quenching can be expected for **BisPhSPCHO** than **PhSPCHO** in solid state.

3-4-2-2 Molecular dipole moments

PhSPDCV
10.59 Debye

PhSPCHO
5.20 Debye

PhSPDPV
0.65 Debye

BisPhSPDCV
14.50 Debye

BisPhSPCHO
7.07 Debye

BisPhSPDPV
0.47 Debye

(a)

$$\mu_{sum} = 2\mu\cos 45°$$

BisPhSPDCV

2 x 10.59 x cos45° = 14.97

BisPhSPCHO

2 x 5.20 x cos45° = 7.35

(b)
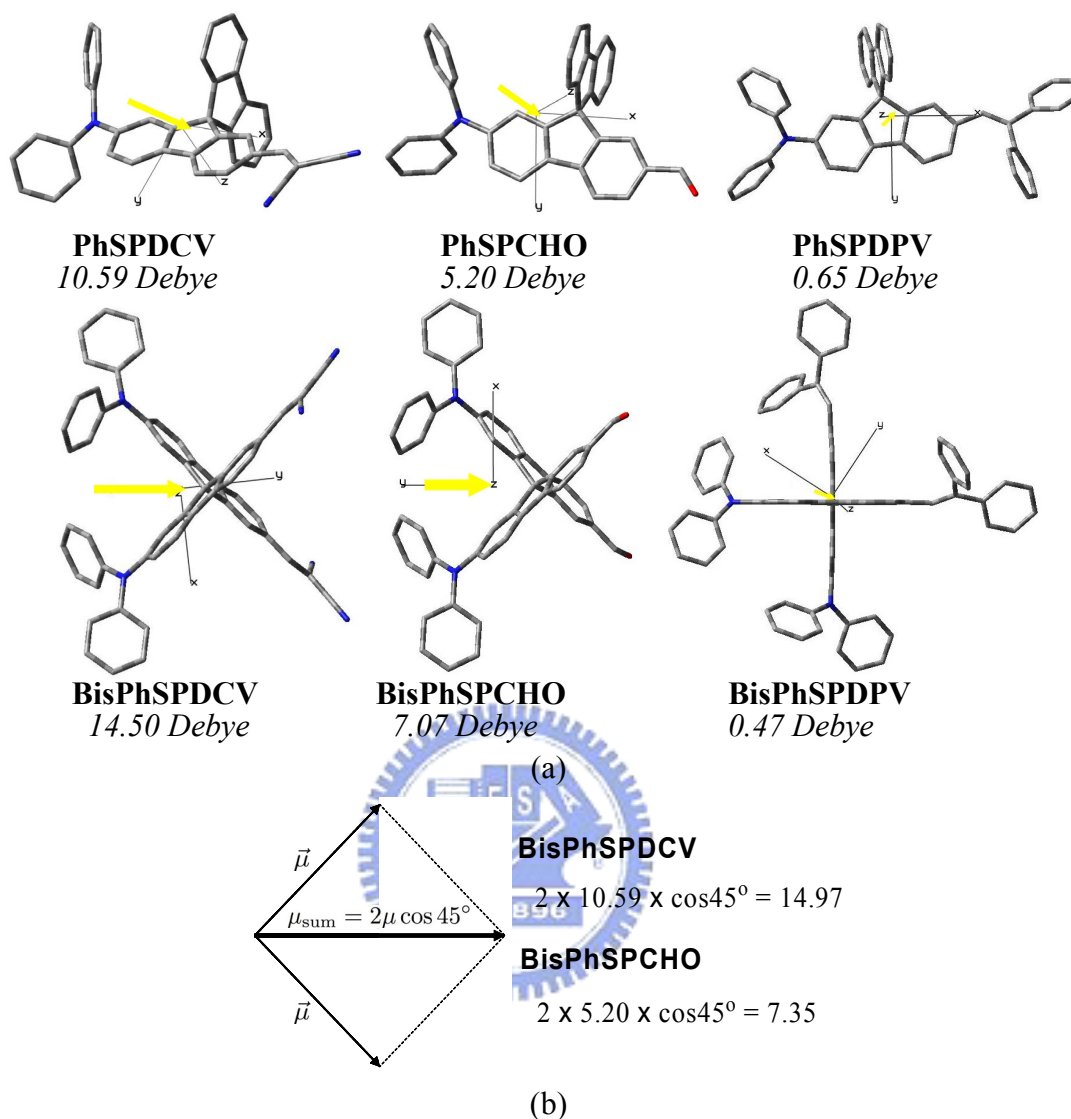
Figure 3-16. (a) Dipole moment in unit of Debye (D) of **PhSPDCV**, **BisPhSPDCV**, **PhSPCHO**, **BisPhSPCHO**, **PhSPDPV** and **BisSPDPV** is labeled in italic fonts, where DFT denotes density function theory and HF denotes Hartree-Fock. The direction and the approximate magnitude of the dipole are illustrated with a yellow arrow. (b) Simple vector analysis of intramolecular dipoles and the net dipole of **BisPhSPDCV** and **BisPhSPCHO** is schematically presented in the bottom.

Molecular dipole moments of these six spiorbifluorenes were estimated by DFT calculation showed in **Figure 3-16**. From theoretical estimation (**Table 3-3**), the ground-state dipole of **BisPhSPDCV** or **BisPhSPCHO** can be considered as the sum of two dipole vectors from two orthogonally aligned molecular halves of **PhSPDCV** or **PhSPCHO**

(**Figure 3-16(b)**).   Based on the DFT-calculated 10.59 Debye of **PhSPDCV** and 5.20 Debye of **PhSPCHO**, a simple method of vector summation leads to 14.95 Debye of **BisPhSPDCV** and 7.35 Debye of **BisPhSPCHO**, which is quite close to 14.50 and 7.07 Debye obtained by DFT/B3LYP calculation, respectively.   However, similar summation method of dipole vectors was less successful in case of **BisPhSPDPV**.   Realizing that **BisPhSPDPV** or **PhSPDPV** does not possess realistic electron withdrawing functionality (diphenylvinyl group is a very weak electronic acceptor), we found that intramolecular dipole vectors of **BisPhSPDPV** are not only small but also disoriented in a non-orthogonal direction (**Figure 3-8**).   The lack of built-in electronic acceptor of the molecule diminishes the electronic push-pull polarization and hence the dipole moment.   On the other hand, dicyanovinyl group of **PhSPDCV** and **BisPhSPDCV** or formyl group of **PhSPCHO** and **BisPhSPCHO** has a strong donor-acceptor pair that greatly polarizes the molecules and leads to a large dipole moment.   Nevertheless, the calculated ground- state dipole moments for "dimeric" **BisPhSPDCV** and **BisPhSPCHO** are larger than those of corresponding "monomeric" molecules **PhSPDCV** and **PhSPCHO**, and this is quite an unusual property.   The Molecular dipole moments of these six spiorbifluorenes play a very important rule in this article.

Table 3-3. Calculated ground state dipole moments and differences in permanent dipole moments of the first excited state and ground state.[a]

	Ground state dipole		First excited state dipole	Difference dipole moment
	μ_{gr}^{DFT}	μ_{gr}^{HF}	μ_{ex}^{CIS}	$\lvert \mu_{ex}^{CIS} - \mu_{gr}^{HF} \rvert$
PhSPDCV	10.59	10.40	16.50	6.14
PhSPCHO	5.20	5.10	9.56	4.46
PhSPDPV	0.65	0.46	2.07	1.66
BisPhSPDCV	14.50	14.05	18.41	4.43
BisPhSPCHO	7.07	6.79	9.97	3.13
BisPhSPDPV	0.47	0.42	1.75	1.35

[a]In Debye.   B3LYP/6-31G* and HF/6-31G* were used for ground state, and CIS/6-31G* for excited state calculations.

3-4-2-3 Optical properties analysis

3-4-2-3-1 Absorption and fluorescence analysis

Table 3-4. Absorption and fluorescence properties.

	Solution		Solid state	
	λ_{max}^{ab}(nm)[a]	λ_{max}^{fl}(nm)[a]	λ_{max}^{ab}(nm)	λ_{max}^{fl}(nm)
PhSPDCV	460	582	498	633
BisPhSPDCV	460	587	499	654
PhSPCHO	400	497	408	502
BisPhSPCHO	401	495	408	508
PhSPDPV	385	468	390	467
BisPhSPDPV	385	468	389	468

[a]**PhSPDPV** and **BisPhSPDPV** were in chlorobenzene; **PhSPDCV**, **BisPhSPDCV**, **PhSPCHO**, and **BisPhSPCHO** were in 1,4-dioxane.

It is anticipated to see that "dimeric" **BisPhSPDCV** possesses very similar energy, either absorption or emission energy, as that of "monomeric" **PhSPDCV** (**Table 3-4**). The same situation was found for **PhSPDPV** and **BisPhSPDPV**, as well as the **PhSPCHO** and **BisPhSPCHO** pair. This perfectly reflects a fact that a sp^3-hibridized carbon in between renders little electronic coupling (π-conjugated interaction) between two donor-acceptor substituted fluorene moieties of the "dimmers". This result is consistent with an earlier report which shows a small interaction (sideways overlapping of π-molecular orbitals) at the spiro-center between the π-electron systems of the two branches.[14, 15, 29]

Changing from solution state to the solid state, only red fluorophores, not blue fluorophores, and to a less extent of green fluorophores, were observed for pronounced bathochromic shifts of λ_{max}^{ab} and λ_{max}^{fl}. Among six spirobifluorene fluorophores, "dimeric" **BisPhSPDCV** exhibited the largest red-shifting of λ_{max}^{ab} from 460 nm in 1,4-dioxane solution to 498 nm in solid state and λ_{max}^{fl} from 587 nm in 1,4-dioxane solution to 654 nm in solid state (**Table 3-4**). Such bathochromic shift of the absorption and emission wavelength of **BisPhSPDCV** is

significantly larger than that of **BisPhSPCHO** or **BisPhSPDPV**.   This is understandable because of the different polarity of three "dimeric" spirobifluorene compounds.   However, we can hardly explain that the bathochromic shifts of "dimeric" **BisPhSPDCV** (or **BisPhSPCHO**) are larger than those of "monomeric" **PhSPDCV** (**PhSPCHO)**.

3-4-2-3-2 Solvatochromic effect

By compare the λ_{max}^{fl} of emission spectra, it is rather similar energy of "dimers" of **BisPhSPDCV**, **BisPhSPCHO**, or **BisPhSPDPV** to the corresponding "monomers", **PhSPDCV**, **PhSPCHO**, or **PhSPDPV**, respectively (**Figure 3-17**).   Among there pairs of spirobifluorene chromophores, both red **PhSPDCV** and **BisPhSPDCV** showed most strong solvatochromic effect of emission from ~560 nm in toluene to ~670 nm in cyanobenzene because of the highly polar molecules.   In solid state, both **PhSPDCV** and **BisPhSPDCV** are situated in an environment (constituted by the spirobifluorene molecules themselves) with higher polarity than in 1,4-dioxane solution and hence red shifting   was observed for both red spirobifluorene compounds (633 and 654 nm, respectively).   Furthermore, since **BisPhSPDCV** has a larger ground-state dipole moment than does **PhSPDCV**, the molecule of **BisPhSPDCV** is thus situated in a more polar environment than is **PhSPDCV** in solid state. Therefore, it is reasonable to see that solid state **BisPhSPDCV** exhibits larger red-shifting of λ_{max}^{fl} than does **PhSPDCV**.   Solid state solvation effect is a well known phenomenon that shifts the emission wavelength of dopant-based OLED.   The λ_{max}^{fl} of blue **PhSPDPV** and **BisPhSPDPV** emission spectra only slightly changed in various solvent due to the almost non-polar structures.   However, the middle solvatochormism results of green **PhSPCHO** and **BisPhSPCHO** were observed due to the middle electronic withdrawing acceptors of formyl groups.   These solvatochormism results imply that the molecular diploe moment of there pairs spirobifluorene compounds in different substantially from each other.
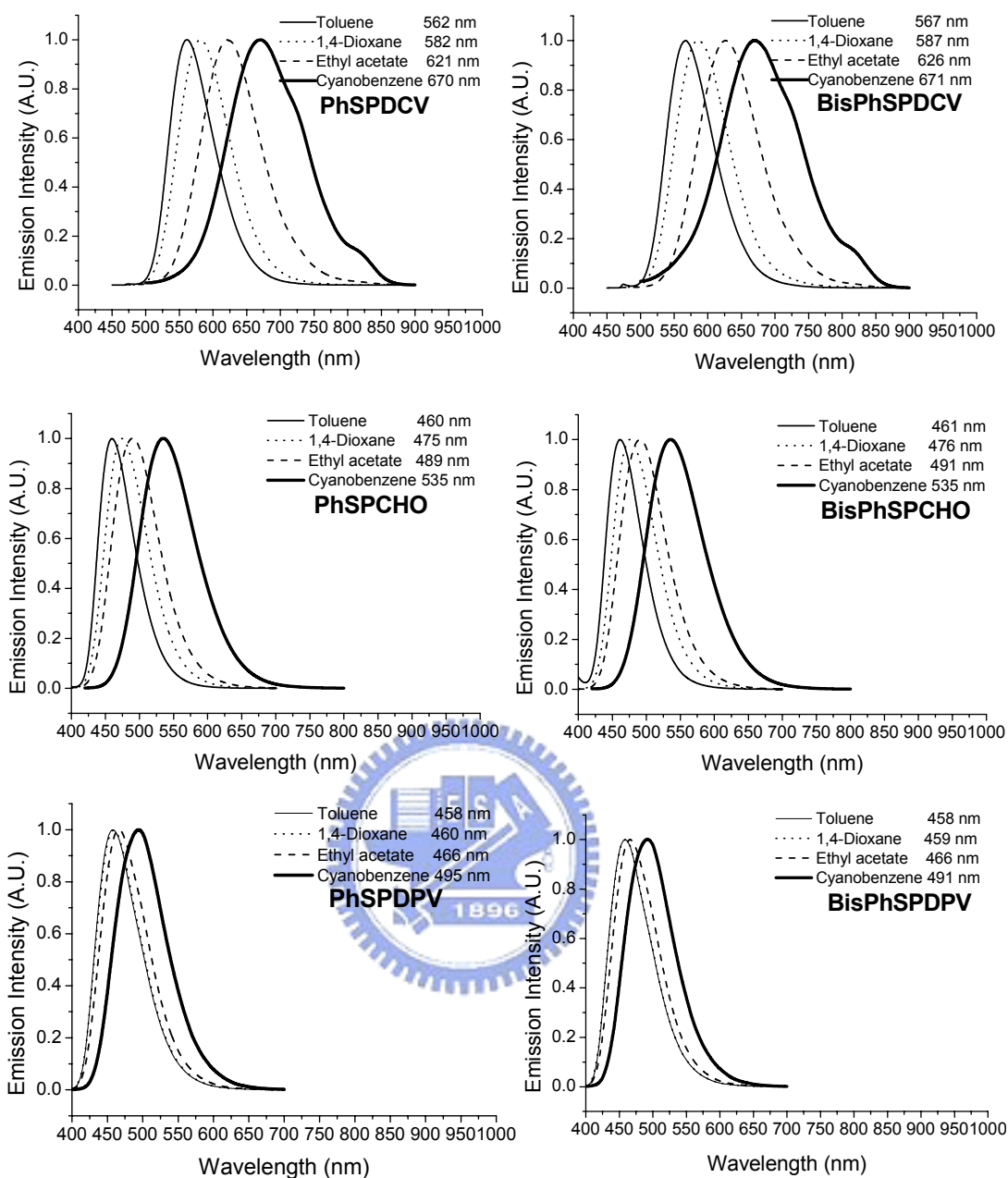
Figure 3-17. Fluorescence spectra of **PhSPDCV**, **BisPhSPDCV**, **PhSPCHO**, **BisPhSPCHO**, **PhSPDPV**, and **BisPhSPDPV** in toluene, 1,4-dioxane, ethyl acetate, and cyanobenzene, respectively.

As shown in **Table 3-3**, the calculated dipole moment difference of ground-state and the first excited- state is large for **PhSPDCV** and **BisPhSPDCV**, medium for **PhSPCHO** and **BisPhSPCHO**, but very small for **PhSPDPV** and **BisPhSPDPV**, is qualitatively consistent with the extent of solvatochromic behavior of these fluorescent spriobifluorenes in solution. Pronounced red-shift by increasing solvent polarity was observed in the fluorescence of large

dipole-bearing **PhSPDCV/BisPhSPDCV** or **PhSPCHO/BisPhSPCHO** (**Figure 3-17**). Similar solvatochromic behavior has been already documented before on other dipolar red fluorophores.[68] The relationship between the dipole moment and solvatochrmism has been described before.[68] Solvatochromism observed here is qualitatively in agreement with the dipole moment changes calculated for **PhSPDCV**, **BisPhSPDCV**, **PhSPCHO** and **BisPhSPCHO** (**Table 3-3**).

3-4-2-3-3 Photoluminescence quantum yield in solution and electric field

Solution fluorescence quantum yields drop from "monomeric" to "dimeric" species, 60-85% decrease for the red **PhSPDCV/BisPhSPDCV,** 50-70% for the green **PhSPCHO/BisPhSPCHO,** and only 10-25% decrease for blue ones (**Table 3-5**). From the single crystal X-ray structures of **PhSPDCV** and **BisPhSPDCV**, no intimate π-π contact was observed in solid state, and therefore we can mostly rule out the fluorescence quenching due to non-emissive excitons arising from π-π stacking. The fluorescence quantum yields decrease as solvent polarity increases, particularly in **PhSPDCV** and **BisPhSPDCV** (**Table 3-5**).

Table 3-5. Solution and solid state photoluminescence quantum yield of six 9'9-spirobifluorene fluorophores

	Φ_f (%)			
	chlorobenzene	1,4-dioxane	ethyl acetate	solid state
PhSPDCV	79	70	49	33
BisPhSPDCV	31	14	7	6
PhSPCHO	83	68	62	42
BisPhSPCHO	49	46	30	10
PhSPDPV	60	60	56	51
BisPhSPDPV	50	54	43	21

The sensitivity of fluorescence quantum yields to the polarity in its surrounding implies that the polar environment may facilitate a non-radiative decay process and lead to

fluorescence quenching. This effect is closely related to a field-induced fluorescence quenching of donor-acceptor- substituted diphenyloligoene fluorophores reported earlier,[30] where an external electric-field with a strength of ~1 MV/cm was applied on the fluorophore-doped polystyrene thin film. It was shown that under an external electric field, fluorescence quenching occurred on the fluorophore with large dipole moment changes between ground and the first excited states. The authors concluded that the external electric-field may lower the energy of a non-emissive intramolecular charge-transfer (ICT) state and it becomes a quenching channel of the light emission. We believe that the electric field, either external or local one, has a great influence on the spirobifluorene fluorophores in the OLEDs studied herein. Light-emitting materials experience an external electric filed of 0.1-1.5 MV/cm (1-15 V applied on the device with ~100 nm thickness), which is comparable with those in reference 30. Moreover, for "dimeric" donor-acceptor-substituted spirobifluorenes, the large ground state dipole moment may generate local electric filed that has an even stronger effect to a nearby molecule or internally to the other molecular half. The strength of the local electric field near a dipole moment can be estimated by

$$E = \frac{1}{4\pi\varepsilon_0 r^3}\left(3(\vec{\mu}\cdot\hat{r})\hat{r} - \vec{\mu}\right) \approx -\frac{\vec{\mu}}{4\pi\varepsilon_0 r^3},$$ (1)

where E is the electric field, $4\pi\varepsilon_0$ is $1.1 \times 10^{-10}\ J^{-1}C^2m^{-1}$, r is the distance to the dipole, μ is the dipole moment in unit of Cm and 1 Debye = $3.34 \times 10^{-30}\ Cm$. In Eq. (1), we have used the field strength at the equatorial plane of the dipole as an estimate. For **BisPhSPDCV**, the edge-to-edge distance between the two molecular halves is about 5 Å. Taking the calculated DFT value of 10 D for **PhDPDCV** as a model for internal dipole moment of the monomer, each molecular halve of **BisPhSPDCV** experiences local electric field from the opposite half of the molecule with a strength of ~12 MV/cm, which is at least an order of magnitude stronger than the external electric field of OLEDs and thus more influential on the fluorescence quenching of the material. For the "monomeric" **PhSPDCV**, there is no

intramolecular electric field but there is an intermolecular effect from neighboring molecules, of which strength of the electric field can be estimated to be as high as 12 MV/cm, assuming the molecular separation distance is 5 Å.   Such a value should be considered as an upper limit of the possible electric field because of possible cancellation of all the surrounding molecular dipoles.   Considering the strength of such electric field falls off quickly as the third power of distance from the molecules, dopant usage can significantly boost the performance of **PhSPDCV** OLEDs but the same approach will be less effective for **PhSPDPV** or **BisPhSPDPV** OLEDs.

For nonpolar blue spirobifluorenes, the solution Φ_f of the blue **BisPhSPDPV** is only about 10-25% smaller than that of **PhSPDPV** in solutions (**Table 3-5**), which is consistent with the small dipole moments of both fluorophores, since they can not generate a local electric field with influential strength. The nonradiative decay due to the higher degree of vibrational motion of the flappy diphenylvinyl groups of **BisPhSPDPV** and **PhSPDPV** is likely to play a more significant role in fluorescence quenching than the effects of dipole moments herein. However, the solid state luminescence yield of **BisPhSPDPV** is almost 60% smaller than that of **PhSPDPV**. We suggest that **BisPhSPDPV** molecules may aggregate in a fashion that favors the solid state fluorescence quenching (due to π-π interaction not intermolecular electric-field) more than does **PhSPDPV**.

The unique structural feature of the donor-acceptor-substituted spirobifluorenes with both "monomeric" and "dimeric" chromophores provides an ideal platform for elucidating the influence of molecular dipole moment on the luminescence quenching.   EL efficiency and the performance of OLEDs are strongly affected by the molecular dipole moment, possibly due to the opening of charge-transfer channels by a local electric field that arises from the molecular dipoles.   In the molecular design of high performance fluorophores for OLEDs, both intramolecular and intermolecular electric field arising from molecular dipole can lead to a reduced luminescence yield and they should be avoided.   This is quite a challenge for the

red light-emitting materials because most of molecular structures of red fluorophores with appreciable intensity of EL are based on donor-acceptor-substituted π-conjugated system, which are dipolar in nature.   Unlike the fluorescence-quenching **BisPhSPDCV**, the good performance of **PhSPDCV**-based non-dopant OLED which showed in Chapter 2 is one rare exception in spite of the large molecular dipole moment.   This is because the bulky and rigid molecular framework of spirobifluorene helps preventing the molecules from close contact. Therefore, the intermolecular electric field strengths are reduced, and the adverse π-π interactions are prevented.

In solid state, the drop of fluorescence quantum yield of these spirobifluorenes was observed, ~80% for red **PhSPDCV**/**BisPhSPDCV**, ~60% for blue **PhSPDPV**/**BisPhSPDPV**. For green **PhSPCHO** and **BisPhSPCHO**, a relatively high ~75% drop of fluorescence quantum yield was observed.   From the single crystal X-ray structures reported previously, no intimate π-π contact was observed for **PhSPDCV** and **BisPhSPDCV** in solid state, so we can mostly rule out the fluorescence quenching due to non-emissive excitons arising from π-π stacking.   However, relatively high ~75% drop of fluorescence quantum yield observed from **PhSPCHO** and **BisPhSPCHO**, it may partially attributed to the detrimental intermolecular π-π contact of **BisPhSPCHO**.   Although, the non-crystallinic amorphous film phase is most suitable for OLEDs, the infrmation of the molecular packing in single crystal provides the worst situation of possible molecular contact in solid film.

3-4-2-3-4 Energy level of spirobifluorenes and their OLED layer structure analysis

Table 3-6. Energy levels of these six spirobifluorene compounds

	ΔE (eV, nm)[c]	HOMO/LUMO (eV/eV)
PhSPDCV	2.41, 514	5.73/3.32
BisPhSPDCV	2.39, 519	5.75/3.36
PhSPCHO	2.83, 438	5.61/2.78
BisPhSPCHO	2.83, 438	5.63/2.80
PhSPDPV	2.91, 426	5.50/2.59
BisPhSPDPV	2.89, 427	5.53/2.64

[c]ΔE is the band-gap energy estimated from the low energy edge of absorption spectra.

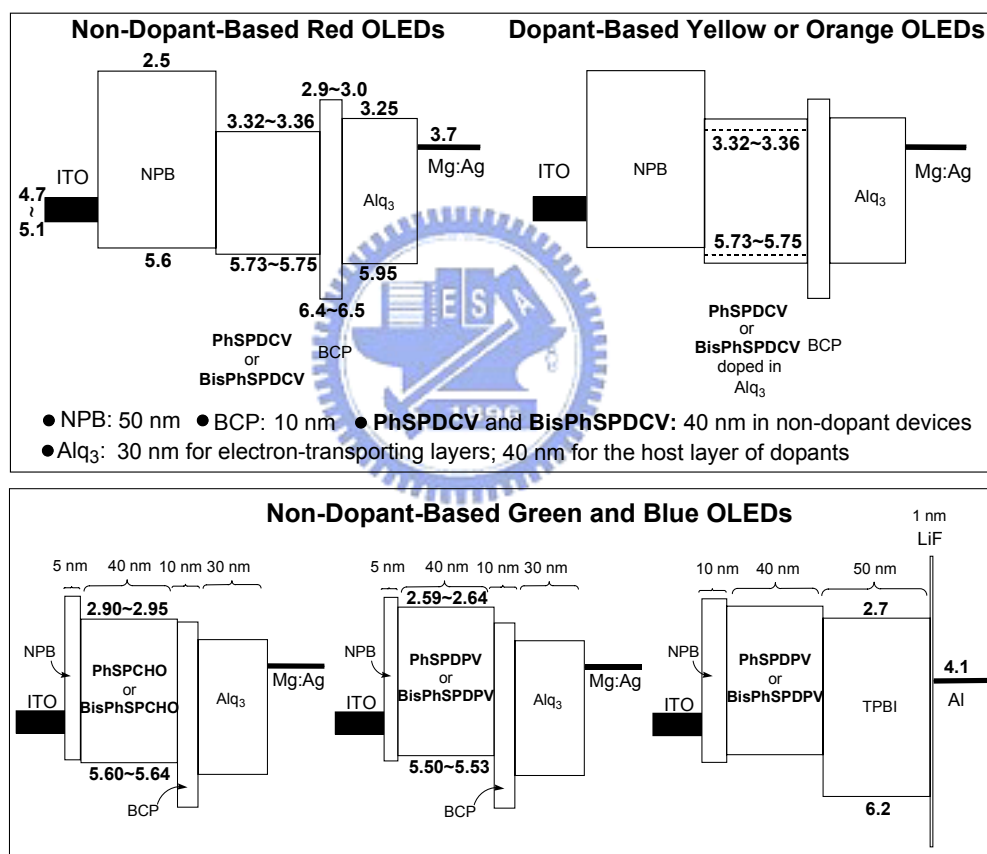**Figure 3-18.** Relative energy-level alignments and layer thickness of OLEDs.

The HOMO energy levels of 9,9'-spirobifluorene compounds were determined by low energy photo-electron spectrometer (AC-2). The numbers of potential energy of HOMO and LUMO levels of the six spirobifluorene compounds are summarized in Table 3-6. Together with other materials adopted in the OLED fabrication, relative energy-level alignments and

layer thickness of OLEDs are schematically depicted in **Figure 3-18**. Since the HOMO energy levels of **PhSPDCV** and **BisPhSPDCV** are rather close (~0.2 eV difference) to that of electron-transporting Alq_3 in OLEDs, a hole blocking layer of BCP was used in either non-dopant or dopant **PhSPDCV** and **BisPhSPDCV** OLEDs (top of **Figure3-18**) to prevent the charge-recombination occurring on Alq_3 that emits undesired green light. A large energy gap (~0.8 eV difference) between the LUMO levels of NPB and **PhSPDCV** (or **BisPhSPDCV**) can effectively confines the electrons inside the light-emitting layer of **PhSPDCV** (or **BisSPDCV**) and facilitates charge recombination that leads to the EL of dopant or non-dopant OLEDs. Within this context, same device configuration, except a thinner NPB layer (5 nm), was adopted for the fabrication of non-dopant **PhSPCHO**, **BisPhSPCHO**, **PhSPDPV**, and **BisPhSPDPV** OLEDs (bottom of **Figure 3-18**). In order to optimize the device structure for higher performance of OLEDs, blue **PhSPDPV** or **BisPhSPDPV** OLEDs was fabricated in another type of configuration: ITO/NPB(10 nm)/**PhSPDPV** or **BisPhSPDPV** (40 nm)/TPBI (50 nm)/LiF(1 nm)/Al (the right figure in the bottom of Figure 3-18). There is no need of BCP herein because of the relatively large difference (~0.7 eV difference) of HOMO energy levels between TPBI and **PhSPDPV** (or **BisPhSPDPV**).

3-4-2-4 Characterization of red, orange and yellow OLEDs

Taking the advantage of double emission density of "dimeric" spirobifluorenes, we want to evaluate the utility of the **BisPhSPDCV** as the non-dopant as well as dopant red emitter for OLEDs. In order to be comparable with each other, the non-dopant-based **PhSPDPV** OLEDs were fabricated again but different device configuration from before was adopted. Accordingly, the dopant-based **PhSPDCV** OLEDs were also fabricated and examined herein for the first time. EL characteristics of dopant- and non-dopant-based **PhSPDCV** and **BisPhSPDCV** OLEDs are shown in **Figure 3-19** and their data are summarized in **Table 3-7**.

Apparently, **BisPhSPDCV** OLEDs performed significantly worse than did **PhSPDCV** OLEDs, either in dopant or non-dopant OLEDs. The only exception to the poor performance of **BisPhSPDCV** is the red color chromaticity. **BisPhSPDCV** OLED has CIE coordinate x = 0.67, y = 0.33 that is redder than CIE coordinate x = 0.65, y = 0.35 of **PhSPDCV** OLED, of which both surpass American or European red color standard of the cathode ray tube (CRT) phosphors (CIE coordinate x = 0.63~0.64, y = 0.33~0.34). Regarding the color chromaticity, it has to note that color chromaticity of both dopant-based **PhSPDCV** or **BisPhSPDCV** OLEDs can not be recognized as red color. In fact, they are saturated yellow, CIE coordinate x = 0.50~0.52, y = 0.47~0.48 (devices with 0.5 wt% dopant concentration) or saturated orange, CIE coordinate x = 0.55~0.59, y = 0.41~0.44 (devices with 3 or 5 wt% dopant concentration) (see **Figure 3-20**). As well known for other red dopant-based OLEDs, the color changing with the variation of the doping concentration of **PhSPDCV** or **BisPhSPDCV** is simply due to the solid-state solvation effect induced by the doping molecules themselves,[31] similar to those observed in solution by the solvent molecules with different polarity (**Figure 3-17**).

Table 3-7. Characteristics of dopant and non-dopant OLEDs of **PhSPDCV**, **BisPhSPDCV**.

	Doping Level of Devices[a] (wt.%)	Max. Luminance (cd/m^2)	Luminance, Efficiency, Voltage (cd/m^2,%, V)[d]	Max. Efficiency (%, cd/A, lm/W)	λ_{max}^{el} (nm)	CIE 1931 Chromaticity (x, y)
I[a]	0.5%	37640	1750, 3.1, 9.1	3.4, 9.4, 8.2	584	0.50, 0.48
II[a]	3%	20950	1080, 2.4, 9.1	2.7, 6.3, 4.1	602	0.55, 0.44
III[a]	100%	8190	3103, 1.4, 6.3	1.5, 1.6, 1.1	634	0.65, 0.35
IV[b]	0.5%	8080	1210, 2.3, 11.3	2.4, 6.4, 4.5	592	0.52, 0.47
V[b]	5%	4290	430, 1.2, 9.1	1.6, 3.0, 2.3	612	0.59, 0.41
VI[b]	100%	2470	90, 0.66, 6.6	0.69, 0.47, 0.22	648	0.67, 0.33

[a]**PhSPDCV**; [b]**BisPhSPDCV**; [c]ITO/NPB(50 nm)/Dopant (x%) in Alq$_3$(40 nm)/BCP(10 nm)/Alq$_3$(30 nm)/Mg:Ag.; [d]At current density of 20 mA/cm^2.
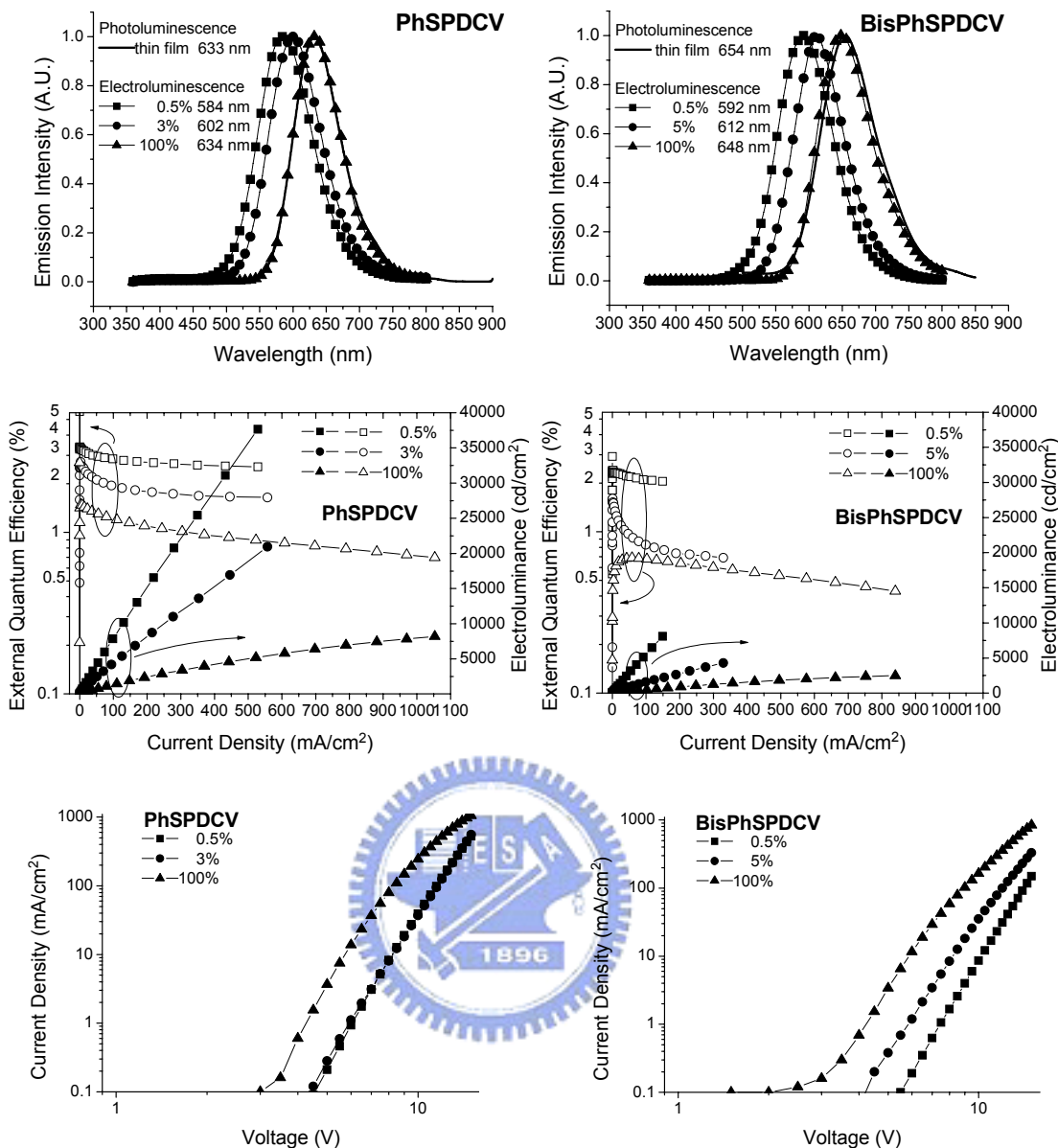
Figure 3-19. Photoluminescence spectra of thin films of **PhSPDCV** and **BisPhSPDCV** compared with EL spectra of corresponding non-dopant and dopant OLEDs.
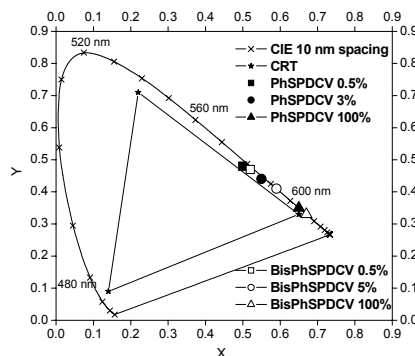

Figure 3-20. 1931 CIE color chromaticity diagram of dopant and non-dopant **PhSPDCV** and **BisPhSPDCV** OLEDs.

OLED performance wise, dopant-based (0.5 wt%) yellow **PhSPDCV** OLED is very efficient and bright, in fact the best of their kind. Its EL efficiency was as high as 3.4%, 9.4 cd/A or 8.2 lm/W, which is better than 8.5 cd/A or 2.8 lm/W of dopant-based yellow *tetra*(*tert*-butylrubrene) OLED,[32] 6.0 cd/A of dopant-based yellow 4-(dicyanomethylene)-2-methyl-6-{2-[4-dimethylamino]phenyl}ethyl}-4*H*-pyan (DCM),[33] and comparable with 3.7%, 10.4 cd/A, or 5.4 lm/W of dopant-based yellow 4-(dicyanomethylene)2-methyl-6-{2-[4-diphenylamino]phenyl}ethyl}-4*H*-pyan (DCM-TPA) OLED.[34] Furthermore, under the current density of 20 mA/cm^2, yellow **PhSPDCV** OLED is as bright as 1750 cd/m^2, which is comparable with 1700 cd/m^2 of *tetra*(*tert*-butylrubrene) yellow OLED[32] and significantly brighter than 1000 and ~1500 cd/m^2 of DCM and DCM-TPA yellow OLED, respectively.[33, 34] The performance (brightness and efficiency) of 0.5 wt% dopant **PhSPDCV** yellow OLED distantly outperforms many other yellow OLEDs (CIE coordinate x = 0.45~0.55, y = 0.45~0.55) that have been documented in the literature.[35, 36] Considering the smaller dipole moment (6 Debye) but better energy alignment (5.56 eV of HOMO and 3.43 eV of LUMO within energy levels of Alq$_3$) of DCM than that of **PhSPDCV**,[34] the suggested strong charge-trapping properties of **PhSPDCV** is probably one of the reasons that **PhSPDCV** yellow OLED outperforms DCM or DCM-TPA yellow OLED. On the other hand, the EL efficiency of rubrene or *tetra*(*tert*-butylrubrene) is supposed to be high. This is because the significantly more spectral overlap between the absorption of rubrene or *tetra*(*tert*-butylrubrene) and the emission of Alq$_3$, when compared with that of DCM or **PhSPDCV** (**Figure 3-21**). In addition, a better HOMO alignment was found for rubrene (5.36 eV) than **PhSPDCV** (5.73 eV) within the host of Alq$_3$ (5.95 eV). We attribute the somewhat low EL efficiency of rubrene type yellow emitters to the poor charge trapping ability of the material, which is in turn ascribed to the small dipole moment nature of such symmetrical and non-polar molecule.
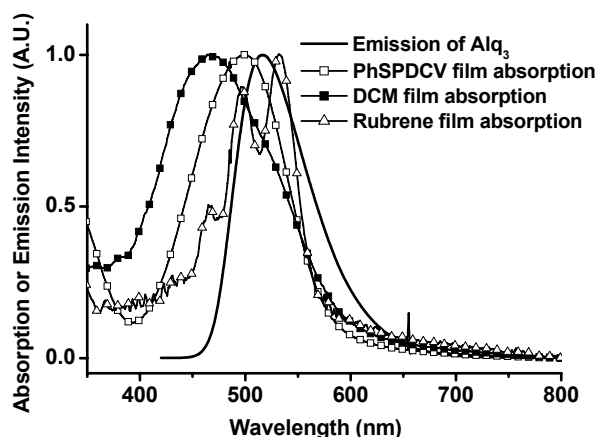
Figure 3-21. Absorption spectra of **PhSPDCV**, DCM, and rubrene and emission spectrum of solid state Alq$_3$.
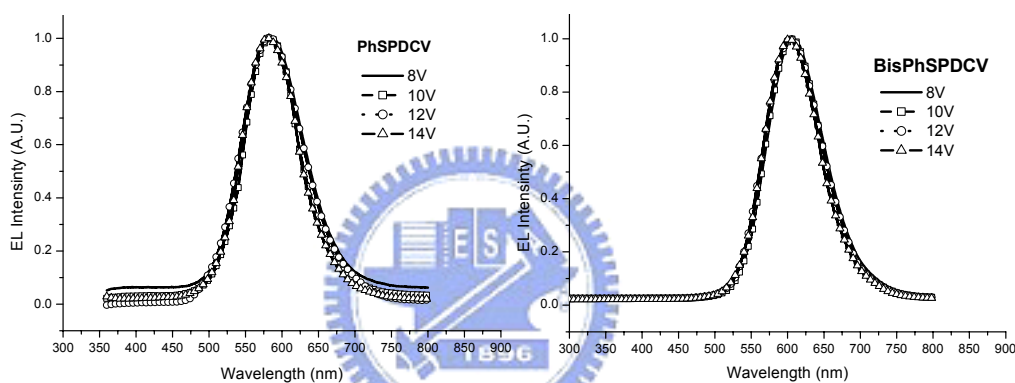
Figure 3-22. The EL spectra of ITO/NPB (50 nm)/red dopant (0.5%) in Alq$_3$ (40 nm)/BCP (10 nm)/Alq$_3$ (30 nm).

There is a well known problem of dopant-based red OLED that EL color will deviate from red to orange or even yellow when the doping concentration is low (usually < 1 or 2 wt%). Recent and previous studies demonstrated that there are two possible origins of such color deviation of red dopant OLED. One is because of the doping-induced charge trapping on the electron-transporting layer, *i.e.*, Alq$_3$.[34] The other is due to the green emission from the host material (Alq$_3$) that is not sufficiently quenched by the red dopant.[31] Whereas the former can be effectively alleviated by adding a hole blocking layer, such as BCP in our devices, in between electron-transporting and doped Alq$_3$ layers, it is hard to find a good method to resolve the latter problem. The most commonly solution is to increase the doping

concentration of red fluorophores but this usually comes with a trouble of concentration quenching of the fluorescent dopant. Such problem does not occur or just happen to a small extent in our case of **PhSPDCV** or **BisPhSPDCV** OLEDs due to the relatively slight concentration quenching of **PhSPDCV** or **BisPhSPDCV** in solid state. There is no Alq$_3$ host-emission of yellow devices at high applied voltage of only 0.5 wt% **PhSPDCV** or **BisPhSPDCV** doping in Alq$_3$ (**Figure 3-22**). In addition, **PhSPDCV** has one more advantage of strong charge-trapping ability due to the large dipole moment. Therefore, highly efficient non-dopant red or dopant yellow OLEDs with high brightness has been achieved with **PhSPDCV**.

3-4-2-5 Non-Dopant Green OLEDs Based on PhSPCHO and BisPhSPCHO as well as Non-dopant Blue OLEDs Based on PhSPDPV and BisPhSPDPV

We attribute the molecular μs to be the major factor that affects the OLED performance of **PhSPDCV** or **BisPhSPDCV**. To further testify such theory, we have prepared the non-dopant OLEDs based on blue fluorophores, **PhSPDPV** and **BisPhSPDPV** as well as green fluorophores, **PhSPCHO** and **BisPhSPCHO**. Their EL were examined and compared with those of **PhSPDCV** and **BisPhSPDCV** OLEDs. Similar to the case of non-dopant **PhSPDCV** and **BisPhSPDCV** OLEDs, **PhSPCHO/BisPhSPCHO** or **PhSPDPV/BisPhSPDPV** exhibited green or blue EL spectra that are nearly coincide with their corresponding photoluminescence ones of thin film state (**Figure 3-23**). This observation indicates that only the green or blue spirobifuirene light-emitting layer contributes to the EL. According to 1931 CIE chromaticity (**Figure 3-24**), **PhSPCHO** or **BisPhSPCHO** OLED is green, whereas **PhSPDPV** or **BisPhSPDPV** OLED is blue in color.
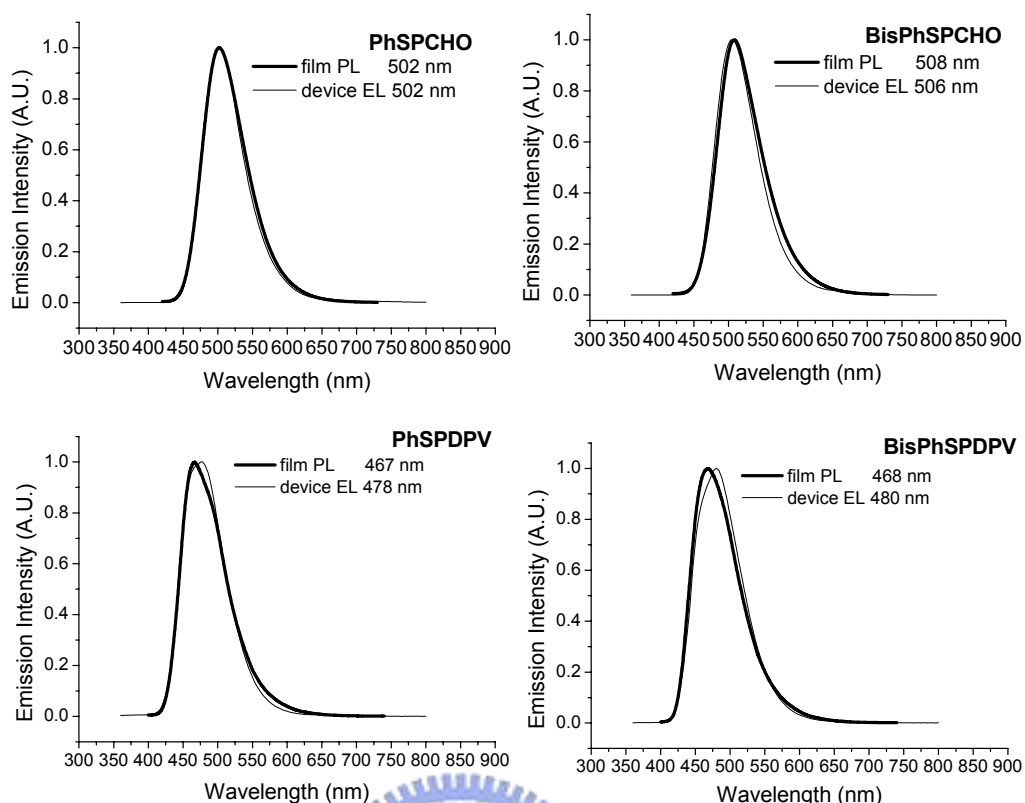
Figure 3-23. Photoluminescence spectra of thin films of **PhSPCHO**, **BisPhSPCHO**, **PhSPDPV**, and **BisSPDPV** compared with EL spectra of corresponding non-dopant OLEDs.
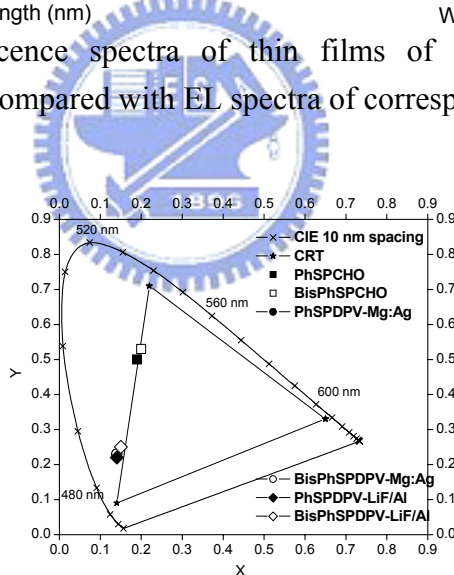
Figure 3-24. 1931 CIE color chromaticity diagram of non-dopant **PhSPCHO**, **BisPhSPCHO**, **PhSPDPV**, and **BisPhSPDPV** OLEDs.

Followifng the point of molecular dipole moment, it is reasonable to observe the difference of EL performance of **PhSPCHO** and **BisPhSPCHO** OLEDs**,** which is still significant but considerably smaller than the difference between **PhSPDCV** and **BisPhSPDCV** OLEDs (see **Figure 3-25** or data in **Table 3-8**).   Nevertheless, as mentioned

above, the face-on π-π interaction found in the x-ray data of **BisPhSPCHO** should be considered as an alternative reason, in addition to the dipole-induced local electric field, for the fluorescence quenching and the worse performance of **BisPhSPCHO** OLED.

Table 3-8. Characteristics of non-dopant OLEDs of PhSPCHO, BisPhSPCHO PhSPDPV, and BisPhSPDPV.

	NPB Layer Thickness (nm)	Max. Luminance (cd/m^2)	Luminance, Efficiency, Voltage $(cd/m^2,\%, V)^c$	Max. Efficiency (%, cd/A, lm/W)	λ_{max}^{el} (nm)	CIE 1931 Chromaticity (x, y)
PhSPCHO	5[a]	33470	1430, 2.6, 7.3	2.7, 7.3, 3.8	502	0.19, 0.50
BisPhSPCHO	5[a]	14600	410, 0.7, 7.5	0.8, 2.4, 0.9	506	0.20, 0.53
PhSPDPV	5[a]	23390	720, 2.2, 6.6	2.2, 3.6, 2.0	470	0.14, 0.23
BisPhSPDPV	5[a]	14380	520, 1.6, 6.9	1.8, 3.0, 1.8	476	0.14, 0.23
PhSPDPV	10[b]	33020	910, 2.9, 4.7	3.4, 5.4, 5.7	478	0.14, 0.22
BisPhSPDPV	10[b]	25470	780, 2.2, 5.1	2.8, 4.9, 5.1	480	0.15, 0.25

[a]Devices have the configuration of ITO/NPB/**PhSPCHO**, **BisSPCHO**, **PhSPDPV**, or **BisPhSPDPV**/BCP/Alq$_3$/Mg:Ag referring to those in **Figure 3-18**. [b] Devices have the configuration of ITO/NPB/**PhSPDPV** or **BisPhSPDPV**/TPBI/LiF/Al referring to those in **Figure 3-18**. [c]At current density of 20 mA/cm^2

Unlike dipolar **PhSPDCV** and **BisPhSPDCV**, **PhSPDPV** and **BisPhSPDPV** are virtually non-polar because of very small dipole moment, 0.65 and 0.47 Debye, respectively. Therefore, the very different OLEDs performance observed for **PhSPDCV** and **BisPhSPDCV** does not occur, or happen to a much smaller extent, in **PhSPDPV** and **BisPhSPDPV** OLEDs (see **Figure 3-24** or data in **Table 3-8**). The dipole moment and local electric field can not account for the relatively worse OLED performance of **BisPhSPDPV** than **PhSPDPV**. As mentioned before, with negligibly small dipole moment, the higher degree of vibrational relaxation of **BisPhSPDPV** molecule and fluorescence concentration quenching (probably due to the unfavored molecular contact in solid state) become the main reason that causes inferior performance of **BisPhSPDPV** OLED.
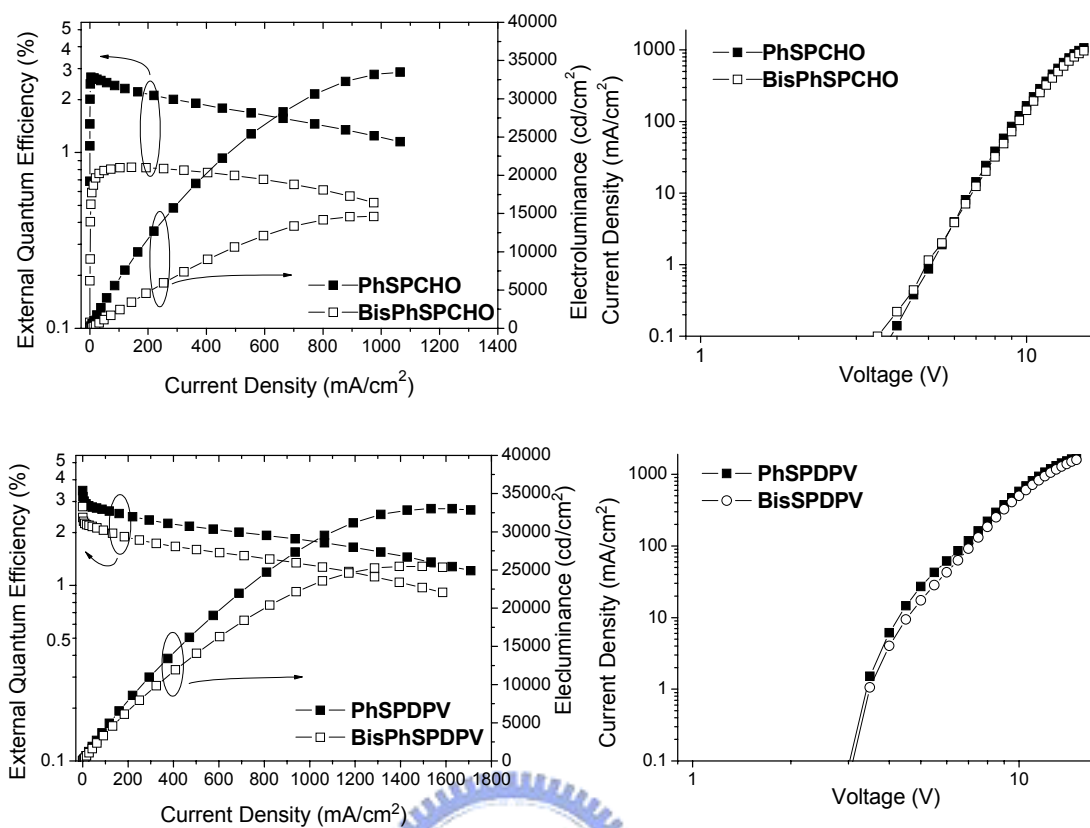
Figure 3-25. Efficiency-current density-electroluminance and current density-voltage characteristics of non-dopant OLEDs based on **PhSPCHO** and **BisSPCHO** (ITO/NPB/**PhSPCHO** or **BisPhSPCHO**/BCP/Alq₃/Mg:Ag) as well as **PhSPDPV** and **BisPhSPDPV** (ITO/NPB/**PhSPDPV** or **BisPhSPDPV**/TPBI/LiF/Al).

We have stressed that the molecular dipole moment plays a major role in affecting the performance of OLEDs based on donor-acceptor-substituted spiro- bifluorene compounds, particularly for the "dimeric" ones. We have also suggested that "dimeric" spirobifluorene compounds, having a nature of larger size of molecular structure than the "monomeric" one, are conceivable to have higher degree of vibrational motion and hence stronger fluorescence quenching. There is one more difference between the "dimeric" and "monomeric" spirobifluorene compounds in the charge recombination and hence EL. "Dimeric" spirobifluorene compounds in principle may have twice a chance better than the "monomeric" spirobifluorene in the capture of electron and hole. However, "dimeric" spirobifluorene compounds also may waste one out of every two times of the charge recombination. This is

because the electron and hole may be trapped separately by different halves of a "dimeric" spirobifluorene molecule, which hampers the subsequent charge recombination because of σ-spiro (π-interrupted) bridge in between the molecular halves. All three possible mechanisms of fluorescence quenching, including the dipole-induced electric field, play their roles in the performance of OLEDs. The issue of the influence of dipole moment on OLEDs has not been addressed before in details until now and we have a very convincing case in illustrating the point.

As far as the performance of blue OLEDs concern, **PhSPDPV** OLED having a configuration of ITO/NPB/**PhSPDPV**/TPBI/LiF/Al is one of the best non-dopant blue electrofluorescence OLEDs. A recent report about non-dopant blue OLED has demonstrated a superb one showing maximum efficiencies of 5.3 cd/A or 3.0 lm/W and maximum brightness of 14300 cd/m^2, which was claimed to be the highest efficiency for blue-light-emitting electrofluorescence OLEDs ever reported, either with or without a dopant (non-dopant) emitter.[4p] Both devices (theirs and ours) exhibit similar blue chromaticity: theirs CIE coordinate x = 0.16, y = 0.22 and ours CIE coordinate x = 0.14, y = 0.22, so both devices can be compared on a fair ground. Our device showed maximum efficiencies of 3.4%, 5.4 cd/A or 5.7 lm/W and maximum brightness of 33020 cd/m^2 (or 910 cd/m^2 at 20 mA/cm^2), which are superior to the one mentioned above. To the best of our knowledge, non-dopant **PhSPDPV** OLED reported herein exhibits the best performance (efficiency, electroluminance, and electroluminance at 20 mA/cm^2) among known dopant- or non-dopant-based electrofluorescence OLEDs with similar blue color purity CIE coordinate x = 0.13-0.18, y = 0.16-0.24.[4b,4d,4h,4j,4m,4o,4p, 37] Within a same range of blue chromaticity, the electroluminance of non-dopant **PhSPDPV** OLED is only next to that of a non-dopant device ITO/DPVSBF/Alq$_3$/LiF/Al,[4m] where DPVSBF is 2,7-bis(2,2-diphenylvinyl)-9,9'-spirobifluorene. Its maximum electroluminance is 41247 cd/m^2 (compared with 33020 cd/m^2 of **PhSPDPV** device) and 928 cd/m^2 (compared with 910 cd/m^2 of **PhSPDPV** device) at 20

mA/cm^2.   However, our **PhSPDPV** device outperforms DPVSBF device in EL efficiency, 3.4 > 3.0%, 5.4 > 5.3 cd/A, or 5.9 > 4.8 lm/W.   Further examination of thermal or morphological stability properties indicates that they are rather comparable with each other: DPVSBF has T_m of 249 ^{o}C, T_c of 161 ^{o}C, T_g of 115 ^{o}C, and T_d of 416 ^{o}C,[4m] and **PhSPDPV** has T_m of 223 ^{o}C, T_g of 112 ^{o}C, and T_d of 405 ^{o}C with the exception of T_c that was not detected for **PhSPDPV** in DSC analysis.   This data imply that **PhSPDPV** should be better than DPVSBF in the thin film morphorlogical stability.   DPVSBF has been proven to be a better material than bench-mark DPVBi (4,4'-bis(2,2-diphenylvinyl)-1,1'-biphenyl)[4p] and we can anticipate a better performance of **PhSPDPV** than DPVSBF, although the relative OLED stability of **PhSPDPV** awaits to be tested.

3-5 Conclusions

Due to the unique structural feature, donor-acceptor-substituted spirobifluorenes including both "monmeric" and "dimeric" ones, provide an ideal model set in elucidating the influence of molecular dipole moment on fluorescence quenching in solution as well as in solid state.   EL and thus the performance of OLEDs are strongly affected by the molecular dipole moment.   In addition to the vibrational motion induced emission quenching and solid state molecule-molecule contact quenching, which are well known reasons of fluorescence quenching, either intramolecular or intermolecular electric field (due to the molecular dipole) is another detrimental factor that should be avoided in the molecular design of high performance fluorophores for OLEDs.   This is quite a challenge for the red (or long wavelength) light-emitting materials because most of molecular structure of red fluorophore with appreciable intensity of electrofluorescence are based on donor-acceptor-substituted π-conjugated system and they are dipolar in nature.   Unlike "dimeric" **BisPhSPDCV**, the very good performance of **PhSPDCV**-based non-dopant OLED is one rare exception, although it has large molecular dipole moment but no problem with fluorescence quenching

due to intramolecular electric filed.   Furthermore, only modest solid state fluorescence quenching was found for **PhSPDCV**, and it is due to the bulky and rigid molecular framework of spirobifluorene that prevents the molecules from close contact and hence reduces the adverse π-π interaction as well as the strength of intermolecular electric field.

In gaining insights into dipole moment properties of these fluorescent materials, we have solved the mystery of why "dimeric" **BisPhSPDCV** (or **BisPhSPCHO**) exhibit significantly worse OLED performance than that of "monomeric" **PhSPDCV** (or **PhSPCHO**) OLED. Consequently, in addition to the high performance of non-dopant red **PhSPDCV** OLEDs, we have successfully achieved one of the best electrofluorescence yellow OLEDs using **PhSPDCV** dopant material.   We have also achieved one of the best electrofluorescence blue OLEDs using the efficient and bright **PhSPDPV** non-dopant material that has practically zero dipole moment and hence no problem with electric-field-induced fluorescence quenching.
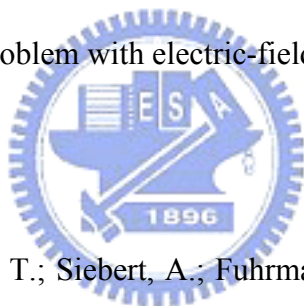
3-6 References

[1] (a) Saragi, T. P. I.; Spehr, T.; Siebert, A.; Fuhrmann-Lieker, T.; Salbeck, J. *Chem. Rev.* **2007**, *101*, 1011.; (b) Wu, R.; Schumm, J. S.; Pearson, D. L.; Tour, J. M. *J. Org. Chem.* **1996**, *61*, 6906.

[2] (a) Fournier, J.-H.; Maris, T.; Wuest, J. D. *J. Org. Chem.* **2004**, *69*, 1762. (b) Demers, E.; Maris, T.; Cabana, J.; Fournier, J.-H.; Wuset, J. D. *Cryst. Growth Design* **2005**, *5*, 1237.

[3] (a) Salbeck, J.; Yu, N.; Bauer, J.; Weissörtel, F.; Bestgen, H. *Synth. Met.* **1997**, *91*, 209.; (b) Salbeck, J.; Weissörtel, F.; Bauer, *J. Macromol. Symp.* **1997**, *125*, 121.; (c) Hohansson, N.; dos Santos, D. A.; Guo, S.; Cornil, J.; Fahlman, M.; Salbeck, J.; Schenk, H.; Arwin, H.; Bredas, J. L.; Salanek, W. R. *J. Chem. Phys.* **1997**, *107*, 2542.; (d) Steuber, F.; Staudigel, J. Stössel, M.; Simmerer, J.; Winnacker, A.; Spreitzer, H.; Weissörtel, F.; Salbeck, J. *Adv. Mater.* **2000**, *12*, 130.; (e) Spehr, T.; Pudzich, R.; Fuhrmann, T.; Salbeck, J. *Org. Electron.* **2003**, *4*, 61.

[4] (a) Lupo, D.; Salbeck, J.; Schenk, H.; Stehlin, T.; Stern, R.; Wolf, A. US Patent 5840217, **1998**.; (b) Kim, Y.-H.; Shin, D.-C.; Kim, S.-H.; Ko, C.-H.; Yu, H.-S.; Chae, Y.-S.; Kwon, S.-K. *Adv. Mater.* **2001**, *13*, 1690.; (c) Geng, Y.; Katsis, D.; Culligan, S. W.; Ou, J. J.; Chen, S. H.; Rothberg, L. J. *Chem. Mater.* **2002**, *14*, 463.; (d) Katsis, D.; Geng, Y. H.; Ou, J. J.; Culligan, S. W.; Trajkovska, Chen, S. H.; Rothberg, L. J. *Chem. Mater.* **2002**, *14*, 1332.; (e) Wu, C.-C.; Lin, Y.-T.; Chiang, H.-H.; Cho, T.-Y.; Chen, C.-W.; Wong, K.-T.; Liao, Y.-L.; Lee, G.-H.; Peng, S.-M. *Appl. Phys. Lett.* **2002**, *81*, 577.; (f) Wong, K.-T.; Chien, Y.-Y.; Chen, R.-T.; Wang, C.-F.; Lin, Y.-T.; Chiang, H.-H.; Hsieh, P.-Y.; Wu, C.-C.; Chou, C.-H.; Su, Y.-O.; Lee, G.-H.; Peng, S.-M. *J. Am. Chem. Soc.* **2002**, *124*, 11576.; (g) Wu, C.-C.; Lin, Y.-T.; Wong, K.-T.; Chen, R.-T.; Chien, Y.-Y. *Adv. Mater.* **2004**, *16*, 61.; (h) Chien, C.-H.; Tao, Y.-T.; Wu, F.-I.; Shu, C.-F. *Appl. Phys. Lett.* **2004**, *85*, 4609.; (i) Wong, K.-T.; Chen, R.-T.; Fang, F.-C.; Wu, C.-C.; Lin, Y.-T. *Org. Lett.* **2005**, *7*, 1979.; (j) Chen, C.-H.; Wu, F.-I.; Shu, C.-F.; Chien, C.-H.; Tao, Y.-T. *J. Mater. Chem.* **2004**, *14*, 1585.; (k) Shen, W.-J.; Dodda, R.; Wu, C.-C.; Wu, F.-I.; Liu, T.-H.; Chen, H.-H.; Chen, C. H.; Shu, C.-F. *Chem. Mater.* **2004**, *16*, 930.; (l) Gebeyehu, D.; Walzer, K.; He, G.; Pfeiffer, M.; Leo, K.; Brandt, J.; Gerhard, A.; Stößel, P.; Vestweber, H. *Synth. Met.* **2005**, *148*, 205.; (m) Wu, F.-I.; Shu, C.-F.; Wang, T.-T.; Diau, E. W.-G.; Chien, C.-H.; Chuen, C.-H.; Tao, Y.-T. *Synth. Met.* **2005**, *151*, 285.; (n) Lee, H.; Oh, J.; Chu, H. Y.; Lee, J.-I.; Kim, S. H.; Yang, Y. S.; Kim, G. H.; Do, L.-M.; Zyung, T.; Lee, J.; Park, Y. *Tetrahedron* **2003**, *59*, 2773.; (o) Shen, J.-Y.; Lee, C.-Y.; Huang, T.-H.; Lin, J.-T.; Tao, Y.-T.; Chien, C.-H.; Tsai, C. *J. Mater. Chem.* **2005**, *15*, 2455.; (p) Tao, S.; Peng, Z.; Zhang, X.; Wang, P.; Lee, C.-S.; Lee, S.-T. *Adv. Funct. Mater.* **2005**, *15*, 1716.

[5] Tour, J. M.; Wu, R.; Schumm, J. S. *J. Am. Chem. Soc.* **1990**, *112*, 5662.

[6] (a) Lupo, D.; Salbeck, J.; Schenk, H.; Stehlin, T.; Stern, R.; Wolf, A. US Patent 5840217, **1998**.; (b) Yu, W. L.; Pei, J.; Huang, W.; Heeger, A. J. *Adv. Mater. (Weinheim, Ger.)*

2000, *12*, 828.; (c) Pei, J.; Ni, J.; Zhou, X. H.; Cao, X. Y.; Lai, Y. H. *J. Org. Chem.* **2002**, *67*, 4924.

[7] Weisburger, J. H.; Weisburger, E. K.; Ray, F. E. *J. Am. Chem. Soc.* **1950**, *72*, 4253.

[8] (a) Prelog, V.; Bedekovic, D. *Hel. Chim. Acta 1979*, **62**, 2285.; (b) Haas, G.; Prelog, V. *Hel. Chim. Acta* **1969**, *52*, 1202.

[9] Schweig, A.; Weidner, U.; Hellwinkel, D.; Krapp, W. *Angew. Chem.* **1973**, *85*, 360.

[10] Pudzich, R.; Fuhrmann-Lieker, T.; Salbeck, J. *Adv. Polym. Sci.* **2006**, *199*, 83.

[11] van Dantzig, N. A.; Levy, D. H.; Vigo, C.; Piotrowiak, P. *J. Chem. Phys.* **1995**, *103*, 4894.

[12] Schartel, B.; Krüger, S.; Wachtendorf, V.; Hennecke, M. *J. Chem. Phys.* **2000**, *112*, 9822.

[13] Yip, W. T.; Levy, D. H.; Kobetic, R.; Piotrowiak, P. *J. Phys. Chem.* A **1999**, *103*, 10.

[14] Johansson, N.; dos Santos, D. A.; Guo, S.; Cornil, J.; Fahlman, M.; Salbeck, J.; Schenk, H.; Arwin, H.; Bredas, J. L.; Salaneck, W. R. *J. Chem. Phys.* **1997**, *107*, 2542.

[15] Wong, K.-T.; Ku, S.-Y.; Cheng, Y.-M.; Lin, X.-Y.; Hung, Y.-Y.; Pu, S.-C.; Chou, P.-T.; Lee, G.-H.; Peng, S.-M. *J. Org. Chem*. **2006**, *71*, 456.

[16] Pudzich, R.; Salbeck, J. *Synth. Met*. **2003**, *138*, 21.

[17] Chen, C.-T. *Chem. Mater.* **2004**, *16*, 4389.

[18] (a) Chien, Y.-Y.; Wong, K.-T.; Chou, P.-T.; Cheng, Y.-M. *Chem. Commun.* **2002**, 2874. ;(b) Wu, C.-C.; Liu, T.-L.; Hung, W.-Y.; Lin, Y.-T.; Wong, K.-T.; Chen, R.-T.; Chen, Y.-M.; Chien, Y.-Y. *J. Am. Chem. Soc.* **2003**, *125*, 3710. ;(c) Müller, C. D.; Falcou, A.; Reckefuss, N.; Rojehn, M.; Eiederhirn, V.; Rudati, P.; Frohne, H.; Nuyken, O.; Becker, H.; Meerholtz, K. *Nature* **2003** *421*, 829.; (d) Schneider, D.; Rabe, T.; Riedl, T.; Dobbertin, T.; Kröger, M.; Becker, E.; Weimann, T.; Wang, J.; Hinze, P. *Appl. Phys. Lett.* **2004**, *85*, 1659.; (e) Su, H.-J.; Wu, F.-I.; Shu, C.-F. *Macromolecules* **2004**, *37*, 7197. ;(f) Wu, Y.; Li, J.; Fu, Y.; Bo, Z. *Org. Lett.* **2004**, *6*, 3485.; (g) Cao, X.-Y.; Zhang,

W.; Zi, H.; Pei, J. *Org. Lett.* **2004**, *6*, 4845.;(h) Cheun, C. H.; Tao, Y. T.; Wu, F. I.; Shu, C. F. *Appl. Phys. Lett.* **2004**, *85*, 4609.; (i) Fungo, F.; Wong, K.-T.; Ku, S.-Y.; Hung, Y.-Y.; Bard, A. J. *J. Phys. Chem. B* **2005**, *109*, 3984.; (j) Oyston, S.; Wang, C.; Hughes, G.; Batsanov, A. S.; Perepichka, I. F.; Bryce, M. R.; Ahn, J. H.; Pearson, C.; Petty, M. C. *J. Mater. Chem.* **2005**, *15*, 194.

[19] Wu, F.-I.; Dodda, R.; Reddy, D. S.; Shu, C.-F. *J. Mater. Chem.* **2002**, *12*, 2893.;

[20] Sutcliffe, F. K.; Shahidi, H. M.; Patterson, D. *J. Soc. Dyes Colors* **1978**, *94*, 306.

[21] Park, J. H.; Ko, H. C.; Kim, J. H.; Lee, H. *Synth. Met*. **2004**, *144*, 193.

[22] (a) Doyle, M. P.; Siegfried, B.; Dellaria, Jr. F. *J. Org. Chem.* **1977**, *42*, 2426.; (b) Doyle, M. P.; Van Lente, M. A.; Mowat, R.; Forbare, W. F. *J. Org. Chem*. **1980**, *45*, 2570.

[23] Becke, A. D. *J. Chem. Phys.* **1993**, *98*, 5648.

[24] Kong, J.; White, C. A.; Krylov, A. I.; Sherrill, D.; Adamson, R. D.; Furlani, T. R.; Lee, M. S.; Lee, A. M.; Gwaltney, S. R.; Adams, T. R.; Ochsenfeld, C.; Gilbert, A. T. B.; Kedziora, G. S.; Rassolov, V. A.; Maurice, D. R.; Nair, N.; Shao, Y. Besley, N. A.; Maslen, P. E.; Dombroski, J. P. Daschel, H.; Zhang, W.; Korambath, P. P.; Baker, J.; Byrd, E. F. C.; Voorhis, T. V.; Oumi, M.; Hirata, S.; Hsu, C.-P.; Ishikawa, N.; Florian, J.; Warshel, A.; Johnson, B. G.; Gill, P. M. W.; Head-Gordon, M.; Pople, J. A. *J. Comput. Chem.* **2000**, *21*, 1532.

[25] Kim, H.-S.; Kim, Y.-H.; Ahn, S.-K.; Kwon, S.-K. *Macromolecules* **2003**, *36*, 2327.

[26] Cheng, X.; Hou, G.-H.; Xie, J.-H.; Zhou, Q.-L. *Org. Lett.* **2004**, *6*, 2381.

[27] Mattiello, L.; Fioravanti, G. *Synth. Commun.* **2001**, *31*, 2645.

[28] Plater, M. J.; Jackson, T.; *Tetrahedron* **2003**, *59*, 4673.

[29] The interaction leads to a small splitting of some orbitals (with reference to the orbitals of two separate molecule halves). The small interaction between the two fluorene halves is also seen in a recent report, in which a photo induced intramolecular electron transfer reaction between the donor and acceptor substituents observed for substituted bipolar spirobifluorene system. It was observed in molecule(s) in which donor and

acceptor were each connected to a fluorene moiety, with a σ-spiro bridge in between. Such electron transfer property is not likely to occur in our system because the charge separation does not usually take place between identical molecular halves. In our system, the donor and acceptor substituents are connected through π-conjugation on the same side of the molecular halves, and the push-pull electronic effect gives rise to the red-shifting of fluorescence.

[30] Nakabayashi, T.; Wahadoszamen, Md.; Ohta, N. *J. Am. Chem. Soc.* **2005**, *127*, 7041.

[31] (a) Tang, C. W.; VanSlyke, S. A.; Chen, C. H. *J. Appl. Phys.* **1989**, *65*, 3610. (b) Bulvić, V.; Deshpande, R.; Thompson, M. E.; Forrest, S. R. *Chem. Phys. Lett.* **1999**, *308*, 317.

[32] (a) Liu, T.-H.; Wu, Y.-S.; Lee, M.-T.; Chen, H.-H.; Liao, C.-H.; Chen, C. H. *Appl. Phys. Lett.* **2004**, *85*, 4304. (b) Wu, Y.-S.; Liu, T.-H.; Chen, H.-H.; Chen, C. H. *Thin Solid Films* **2006**, *496*, 626.

[33] Xie, Z. Y.; Hung, L. S.; Lee, S. T. *Appl. Phys. Lett.* **2001**, *79*, 1048.

[34] Nüesch, F.; Berner, D.; Tutiš, E.; Schaer, M.; Ma, C.; Wang, X.; Zhang, B.; Zuppiroli, L. *Adv. Funct. Mater.* **2005**, *15*, 323.

[35] Bulvić, V.; Shoustikov, A.; Baldo, M. A.; Bose, E.; Kozlov, V. G.; Thompson, M. E.; Forrest, S. R. *Chem. Phys. Lett.* **1998**, *287*, 455.

[36] (a) Lin, X. Q.; Chen, B. J.; Zhang, X. H.; Lee, C. S.; Kwong, H. L.; Lee, S. T. *Chem. Mater.* **2001**, *13*, 456.; (b) Thomas, K. R. J.; Lin, J. T.; Tao, Y.-T.; Chuen, C.-H. *Chem. Mater.* **2002**, *14*, 2796.; (c) Thomas, K. R. J.; Lin, J. T.; Tao, Y.-T.; Chuen, C.-H.; *J. Mater. Chem.* **2002**, *12*, 3516.; (d) Thomas, K. R. J.; Lin, J. T.; Tao, Y.-T.; Chuen, C.-H.; *J. Mater. Chem.* **2002**, *12*, 3852.; (e) Xie, W.-F.; Li, C.-N.; Liu, S.-Y. *Chin. Phys. Lett.* **2003**, *20*, 956.; (f) Chen, H.-Y.; Chi, Y.; Liu, C.-S.; Yu, J.-K.; Cheng, Y.-M.; Chen, K.-S.; Chou, P.-T.; Peng, S.-M.; Lee, G.-H.; Carty, A. J.; Yeh, S.-J.; Chen, C.-T. *Adv. Mater.* **2005**, *15*, 567.; (g) Lee, J.; Yuan, Y.-Y.; Kang, Y.; Jia, W.-L.; Lu, Z.-H.; Wang, S. *Adv. Funct.. Mater.* **2006**, *16*, 681.

[37] (a) Danel, K.; Huang, T.-H.; Lin, J. T.; Tao, Y.-T.; Chuen, C.-H. *Chem. Mater.* **2002**, *14*, 3860.; (b) Guan, M.; Bian, Z. Q.; Zhou, Y. F.; Li, F. Y.; Li, Z. J.; Huang, C. H. *Chem.*

Commun. **2003**, 2708.; (c) Thomas, K. R. J.; Lin, J. T.; Tao, Y.-T.; Chien, C.-H. *Adv. Funct. Mater.* **2003**, *13*, 445.; (c) Thomas, K. R. J.; Velusamy, M.; Lin, J. T.; Chien, C.-H.; Tao, Y.-T. *J. Mater. Chem.* **2005**, *15*, 4453.; (d) Wu, F.-I.; Shih, P.-I.; Yuan, M.-C.; Dixit, A. K.; Shu, C.-F.; Chung, Z.-M.; Diau, E. W.-G. *J. Mater. Chem.* **2005**, *15*, 4753.; (e) Tseng, R. J.; Chiechi, R. C.; Wudl, F.; Yang, Y. *Appl. Phys. Lett.* **2006**, *88*, 093512.; (f) Tang, C.; Liu, F.; Xia, Y.-J.; Lin, J.; Xie, L.-H.; Zhong, G.-Y.; Fan, Q.-L.; Huang, W. *Org. Electron.* **2006**, *7*, 155.; (g) Chiechi, R. C.; Tseng, R. J.; Marchioni, F.; Yang, Y.; Wudl, F. *Adv. Mater.* **2006**, *18*, 325.

[38] (a) Saragi, T. P. I.; Spehr, T.; Siebert, A.; Fuhrmann-Lieker, T.; Salbeck, J. *Chem. Rev.* **2007**, *101*, 1011.; (b) Wu, R.; Schumm, J. S.; Pearson, D. L.; Tour, J. M. *J. Org. Chem.* **1996**, *61*, 6906.

[39] (a) Fournier, J.-H.; Maris, T.; Wuest, J. D. *J. Org. Chem.* **2004**, *69*, 1762. (b) Demers, E.; Maris, T.; Cabana, J.; Fournier, J.-H.; Wuset, J. D. *Cryst. Growth Design* **2005**, *5*, 1237.

[40] (a) Salbeck, J.; Yu, N.; Bauer, J.; Weissörtel, F.; Bestgen, H. *Synth. Met.* **1997**, *91*, 209.; (b) Salbeck, J.; Weissörtel, F.; Bauer, J. *Macromol. Symp.* **1997**, *125*, 121.; (c) Hohansson, N.; dos Santos, D. A.; Guo, S.; Cornil, J.; Fahlman, M.; Salbeck, J.; Schenk, H.; Arwin, H.; Bredas, J. L.; Salanek, W. R. *J. Chem. Phys.* **1997**, *107*, 2542.; (d) Steuber, F.; Staudigel, J.; Stössel, M.; Simmerer, J.; Winnacker, A.; Spreitzer, H.; Weissörtel, F.; Salbeck, J. *Adv. Mater.* **2000**, *12*, 130.; (e) Spehr, T.; Pudzich, R.; Fuhrmann, T.; Salbeck, J. *Org. Electron.* **2003**, *4*, 61.

[41] (a) Lupo, D.; Salbeck, J.; Schenk, H.; Stehlin, T.; Stern, R.; Wolf, A. US Patent 5840217, **1998**.; (b) Kim, Y.-H.; Shin, D.-C.; Kim, S.-H.; Ko, C.-H.; Yu, H.-S.; Chae, Y.-S.; Kwon, S.-K. *Adv. Mater.* **2001**, *13*, 1690.; (c) Geng, Y.; Katsis, D.; Culligan, S. W.; Ou, J. J.; Chen, S. H.; Rothberg, L. J. *Chem. Mater.* **2002**, *14*, 463.; (d) Katsis, D.; Geng, Y. H.; Ou, J. J.; Culligan, S. W.; Trajkovska, Chen, S. H.; Rothberg, L. J. *Chem. Mater.* **2002**, *14*, 1332.; (e) Wu, C.-C.; Lin, Y.-T.; Chiang, H.-H.; Cho, T.-Y.; Chen, C.-W.; Wong,

K.-T.; Liao, Y.-L.; Lee, G.-H.; Peng, S.-M. *Appl. Phys. Lett.* **2002**, *81*, 577.; (f) Wong, K.-T.; Chien, Y.-Y.; Chen, R.-T.; Wang, C.-F.; Lin, Y.-T.; Chiang, H.-H.; Hsieh, P.-Y.; Wu, C.-C.; Chou, C.-H.; Su, Y.-O.; Lee, G.-H.; Peng, S.-M. *J. Am. Chem. Soc.* **2002**, *124*, 11576.; (g) Wu, C.-C.; Lin, Y.-T.; Wong, K.-T.; Chen, R.-T.; Chien, Y.-Y. *Adv. Mater.* **2004**, *16*, 61.; (h) Chien, C.-H.; Tao, Y.-T.; Wu, F.-I.; Shu, C.-F. *Appl. Phys. Lett.* **2004**, *85*, 4609.; (i) Wong, K.-T.; Chen, R.-T.; Fang, F.-C.; Wu, C.-C.; Lin, Y.-T. *Org. Lett.* **2005**, *7*, 1979.; (j) Chen, C.-H.; Wu, F.-I.; Shu, C.-F.; Chien, C.-H.; Tao, Y.-T. *J. Mater. Chem.* **2004**, *14*, 1585.; (k) Shen, W.-J.; Dodda, R.; Wu, C.-C.; Wu, F.-I.; Liu, T.-H.; Chen, H.-H.; Chen, C. H.; Shu, C.-F. *Chem. Mater.* **2004**, *16*, 930.; (l) Gebeyehu, D.; Walzer, K.; He, G.; Pfeiffer, M.; Leo, K.; Brandt, J.; Gerhard, A.; Stößel, P.; Vestweber, H. *Synth. Met.* **2005**, *148*, 205.; (m) Wu, F.-I.; Shu, C.-F.; Wang, T.-T.; Diau, E. W.-G.; Chien, C.-H.; Chuen, C.-H.; Tao, Y.-T. *Synth. Met.* **2005**, *151*, 285.; (n) Lee, H.; Oh, J.; Chu, H. Y.; Lee, J.-I.; Kim, S. H.; Yang, Y. S.; Kim, G. H.; Do, L.-M.; Zyung, T.; Lee, J.; Park, Y. *Tetrahedron* **2003**, *59*, 2773.; (o) Shen, J.-Y.; Lee, C.-Y.; Huang, T.-H.; Lin, J.-T.; Tao, Y.-T.; Chien, C.-H.; Tsai, C. *J. Mater. Chem.* **2005**, *15*, 2455.; (p) Tao, S.; Peng, Z.; Zhang, X.; Wang, P.; Lee, C.-S.; Lee, S.-T. *Adv. Funct. Mater.* **2005**, *15*, 1716.

[42] Tour, J. M.; Wu, R.; Schumm, J. S. *J. Am. Chem. Soc.* **1990**, *112*, 5662.

[43] (a) Lupo, D.; Salbeck, J.; Schenk, H.; Stehlin, T.; Stern, R.; Wolf, A. US Patent 5840217, **1998**.; (b) Yu, W. L.; Pei, J.; Huang, W.; Heeger, A. J. *Adv. Mater. (Weinheim, Ger.)* **2000**, *12*, 828.; (c) Pei, J.; Ni, J.; Zhou, X. H.; Cao, X. Y.; Lai, Y. H. *J. Org. Chem.* **2002**, *67*, 4924.

[44] Weisburger, J. H.; Weisburger, E. K.; Ray, F. E. *J. Am. Chem. Soc.* **1950**, *72*, 4253.

[45] (a) Prelog, V.; Bedekovic, D. *Hel. Chim. Acta 1979*, **62**, 2285.; (b) Haas, G.; Prelog, V. *Hel. Chim. Acta* **1969**, *52*, 1202.

[46] Schweig, A.; Weidner, U.; Hellwinkel, D.; Krapp, W. *Angew. Chem.* **1973**, *85*, 360.

[47] Pudzich, R.; Fuhrmann-Lieker, T.; Salbeck, J. *Adv. Polym. Sci.* **2006**, *199*, 83.

[48] van Dantzig, N. A.; Levy, D. H.; Vigo, C.; Piotrowiak, P. *J. Chem. Phys.* **1995**, *103*, 4894.

[49] Schartel, B.; Krüger, S.; Wachtendorf, V.; Hennecke, M. *J. Chem. Phys.* **2000**, *112*, 9822.

[50] Yip, W. T.; Levy, D. H.; Kobetic, R.; Piotrowiak, P. *J. Phys. Chem.* A **1999**, *103*, 10.

[51] Johansson, N.; dos Santos, D. A.; Guo, S.; Cornil, J.; Fahlman, M.; Salbeck, J.; Schenk, H.; Arwin, H.; Brédas, J. L.; Salaneck, W. R. *J. Chem. Phys.* **1997**, *107*, 2542.

[52] Wong, K.-T.; Ku, S.-Y.; Cheng, Y.-M.; Lin, X.-Y.; Hung, Y.-Y.; Pu, S.-C.; Chou, P.-T.; Lee, G.-H.; Peng, S.-M. *J. Org. Chem.* **2006**, *71*, 456.

[53] Pudzich, R.; Salbeck, J. *Synth. Met.* **2003**, *138*, 21.

[54] Chen, C.-T. *Chem. Mater.* **2004**, *16*, 4389.

[55] (a) Chien, Y.-Y.; Wong, K.-T.; Chou, P.-T.; Cheng, Y.-M. *Chem. Commun.* **2002**, 2874. ;(b) Wu, C.-C.; Liu, T.-L.; Hung, W.-Y.; Lin, Y.-T.; Wong, K.-T.; Chen, R.-T.; Chen, Y.-M.; Chien, Y.-Y. *J. Am. Chem. Soc.* **2003**, *125*, 3710. ;(c) Müller, C. D.; Falcou, A.; Reckefuss, N.; Rojehn, M.; Eiederhirn, V.; Rudati, P.; Frohne, H.; Nuyken, O.; Becker, H.; Meerholtz, K. *Nature* **2003** *421*, 829.; (d) Schneider, D.; Rabe, T.; Riedl, T.; Dobbertin, T.; Kröger, M.; Becker, E.; Weimann, T.; Wang, J.; Hinze, P. *Appl. Phys. Lett.* **2004**, *85*, 1659.; (e) Su, H.-J.; Wu, F.-I.; Shu, C.-F. *Macromolecules* **2004**, *37*, 7197. ;(f) Wu, Y.; Li, J.; Fu, Y.; Bo, Z. *Org. Lett.* **2004**, *6*, 3485.; (g) Cao, X.-Y.; Zhang, W.; Zi, H.; Pei, J. *Org. Lett.* **2004**, *6*, 4845.;(h) Cheun, C. H.; Tao, Y. T.; Wu, F. I.; Shu, C. F. *Appl. Phys. Lett.* **2004**, *85*, 4609.; (i) Fungo, F.; Wong, K.-T.; Ku, S.-Y.; Hung, Y.-Y.; Bard, A. J. *J. Phys. Chem. B* **2005**, *109*, 3984.; (j) Oyston, S.; Wang, C.; Hughes, G.; Batsanov, A. S.; Perepichka, I. F.; Bryce, M. R.; Ahn, J. H.; Pearson, C.; Petty, M. C. *J. Mater. Chem.* **2005**, *15*, 194.

[56] Wu, F.-I.; Dodda, R.; Reddy, D. S.; Shu, C.-F. *J. Mater. Chem.* **2002**, *12*, 2893.;

[57] Sutcliffe, F. K.; Shahidi, H. M.; Patterson, D. *J. Soc. Dyes Colors* **1978**, *94*, 306.

[58] Park, J. H.; Ko, H. C.; Kim, J. H.; Lee, H. *Synth. Met.* **2004**, *144*, 193.

[59] (a) Doyle, M. P.; Siegfried, B.; Dellaria, Jr. F. *J. Org. Chem.* **1977**, *42*, 2426.; (b) Doyle, M. P.; Van Lente, M. A.; Mowat, R.; Forbare, W. F. *J. Org. Chem.* **1980**, *45*, 2570.

[60] Becke, A. D. *J. Chem. Phys.* **1993**, *98*, 5648.

[61] Kong, J.; *et al. J. Comput. Chem.* **2000**, *21*, 1532.

[62] Kim, H.-S.; Kim, Y.-H.; Ahn, S.-K.; Kwon, S.-K. *Macromolecules* **2003**, *36*, 2327.

[63] Cheng, X.; Hou, G.-H.; Xie, J.-H.; Zhou, Q.-L. *Org. Lett.* **2004**, *6*, 2381.

[64] Mattiello, L.; Fioravanti, G. *Synth. Commun.* **2001**, *31*, 2645.

[65] Plater, M. J.; Jackson, T. *Tetrahedron* **2003**, *59*, 4673.

[66] The interaction leads to a small splitting of some orbitals (with reference to the orbitals of two separate molecule halves). The small interaction between the two fluorene halves is also seen in a recent report, in which a photo induced intramolecular electron transfer reaction between the donor and acceptor substituents observed for substituted bipolar spirobifluorene system. It was observed in molecule(s) in which donor and acceptor were each connected to a fluorene moiety, with a σ-spiro bridge in between. Such electron transfer property is not likely to occur in our system because the charge separation does not usually take place between identical molecular halves. In our system, the donor and acceptor substituents are connected through π-conjugation on the same side of the molecular halves, and the push-pull electronic effect gives rise to the red-shifting of fluorescence.

[67] Nakabayashi, T.; Wahadoszamen, Md.; Ohta, N. *J. Am. Chem. Soc.* **2005**, *127*, 7041.

[68] (a) Tang, C. W.; VanSlyke, S. A.; Chen, C. H. *J. Appl. Phys.* **1989**, *65*, 3610. (b) Bulvić, V.; Deshpande, R.; Thompson, M. E.; Forrest, S. R. *Chem. Phys. Lett.* **1999**, *308*, 317.

[69] (a) Liu, T.-H.; Wu, Y.-S.; Lee, M.-T.; Chen, H.-H.; Liao, C.-H.; Chen, C. H. *Appl. Phys. Lett.* **2004**, *85*, 4304. (b) Wu, Y.-S.; Liu, T.-H.; Chen, H.-H.; Chen, C. H. *Thin Solid Films* **2006**, *496*, 626.

[70] Xie, Z. Y.; Hung, L. S.; Lee, S. T. *Appl. Phys. Lett.* **2001**, *79*, 1048.

[71] Nüesch, F.; Berner, D.; Tutiš, E.; Schaer, M.; Ma, C.; Wang, X.; Zhang, B.; Zuppiroli, L. *Adv. Funct. Mater.* **2005**, *15*, 323.

[72] Bulvić, V.; Shoustikov, A.; Baldo, M. A.; Bose, E.; Kozlov, V. G.; Thompson, M. E.; Forrest, S. R. *Chem. Phys. Lett.* **1998**, *287*, 455.

[73] (a) Lin, X. Q.; Chen, B. J.; Zhang, X. H.; Lee, C. S.; Kwong, H. L.; Lee, S. T. *Chem. Mater.* **2001**, *13*, 456.; (b) Thomas, K. R. J.; Lin, J. T.; Tao, Y.-T.; Chuen, C.-H. *Chem. Mater.* **2002**, *14*, 2796.; (c) Thomas, K. R. J.; Lin, J. T.; Tao, Y.-T.; Chuen, C.-H.; *J. Mater. Chem.* **2002**, *12*, 3516.; (d) Thomas, K. R. J.; Lin, J. T.; Tao, Y.-T.; Chuen, C.-H.; *J. Mater. Chem.* **2002**, *12*, 3852.; (e) Xie, W.-F.; Li, C.-N.; Liu, S.-Y. *Chin. Phys. Lett.* **2003**, *20*, 956.; (f) Chen, H.-Y.; Chi, Y.; Liu, C.-S.; Yu, J.-K.; Cheng, Y.-M.; Chen, K.-S.; Chou, P.-T.; Peng, S.-M.; Lee, G.-H.; Carty, A. J.; Yeh, S.-J.; Chen, C.-T. *Adv. Mater.* **2005**, *15*, 567.; (g) Lee, J.; Yuan, Y.-Y.; Kang, Y.; Jia, W.-L.; Lu, Z.-H.; Wang, S. *Adv. Funct.. Mater.* **2006**, *16*, 681.

[74] (a) Danel, K.; Huang, T.-H.; Lin, J. T.; Tao, Y.-T.; Chuen, C.-H. *Chem. Mater.* **2002**, *14*, 3860.; (b) Guan, M.; Bian, Z. Q.; Zhou, Y. F.; Li, F. Y.; Li, Z. J.; Huang, C. H. *Chem. Commun.* **2003**, 2708.; (c) Thomas, K. R. J.; Lin, J. T.; Tao, Y.-T.; Chien, C.-H. *Adv. Funct. Mater.* **2003**, *13*, 445.; (c) Thomas, K. R. J.; Velusamy, M.; Lin, J. T.; Chien, C.-H.; Tao, Y.-T. *J. Mater. Chem.* **2005**, *15*, 4453.; (d) Wu, F.-I.; Shih, P.-I.; Yuan, M.-C.; Dixit, A. K.; Shu, C.-F.; Chung, Z.-M.; Diau, E. W.-G. *J. Mater. Chem.* **2005**, *15*, 4753.; (e) Tseng, R. J.; Chiechi, R. C.; Wudl, F.; Yang, Y. *Appl. Phys. Lett.* **2006**, *88*, 093512.; (f) Tang, C.; Liu, F.; Xia, Y.-J.; Lin, J.; Xie, L.-H.; Zhong, G.-Y.; Fan, Q.-L.; Huang, W. *Org. Electron.* **2006**, *7*, 155.; (g) Chiechi, R. C.; Tseng, R. J.; Marchioni, F.; Yang, Y.; Wudl, F. *Adv. Mater.* **2006**, *18*, 325.